National Park Service
U.S. Department of the Interior

Natural Resource Stewardship and Science

Surficial Geology and Proglacial Lake Change at Sít' Tlein (Malaspina Glacier), Wrangell-St. Elias National Park and Preserve, Alaska

Natural Resource Report NPS/WRST/NRR—2024/2620

ON THIS PAGE
Fluted moraines in the Sít' Tlein foreland just west of Malaspina Lake. View to the northwest.
NPS / ANNA THOMPSON

ON THE COVER
A portion of Sít' Tlein as seen from a passing commercial aircraft. Ice flows into the photo from the top of the picture. Proglacial lakes, the debris-covered terminus, and the vegetated glacier foreland are visible at lower left. View to the north.
NPS / MICHAEL LOSO.

Surficial Geology and Proglacial Lake Change at Sít' Tlein (Malaspina Glacier), Wrangell-St. Elias National Park and Preserve, Alaska

Natural Resource Report NPS/WRST/NRR—2024/2620

Anna C. Thompson[1], Michael G. Loso[1], Sydney A. Mooneyham[2], Brandon S. Tober[3], Christopher F. Larsen[4], John W. Holt[2,3]

[1] Wrangell-St. Elias National Park and Preserve
PO Box 439
Copper Center, Alaska 99573

[2] University of Arizona
Lunar and Planetary Laboratory
1629 E. University Blvd.
Tucson, Arizona 85721

[3] University of Arizona
Department of Geosciences
1040 E. 4th Street
Tucson, Arizona 85721

[4] Geophysical Institute
University of Alaska Fairbanks
Fairbanks AK 99775

January 2024

U.S. Department of the Interior
National Park Service
Natural Resource Stewardship and Science
Fort Collins, Colorado

The National Park Service, Natural Resource Stewardship and Science office in Fort Collins, Colorado, publishes a range of reports that address natural resource topics. These reports are of interest and applicability to a broad audience in the National Park Service and others in natural resource management, including scientists, conservation and environmental constituencies, and the public.

The Natural Resource Report Series is used to disseminate comprehensive information and analysis about natural resources and related topics concerning lands managed by the National Park Service. The series supports the advancement of science, informed decision-making, and the achievement of the National Park Service mission. The series also provides a forum for presenting more lengthy results that may not be accepted by publications with page limitations.

All manuscripts in the series receive the appropriate level of peer review to ensure that the information is scientifically credible and technically accurate.

Views, statements, findings, conclusions, recommendations, and data in this report do not necessarily reflect views and policies of the National Park Service, U.S. Department of the Interior. Mention of trade names or commercial products does not constitute endorsement or recommendation for use by the U.S. Government.

This report is available in digital format from and the Natural Resource Publications Management website. If you have difficulty accessing information in this publication, particularly if using assistive technology, please email irma@nps.gov.

Please cite this publication as:

Thompson, A. C., M. G. Loso, S. A. Mooneyham, B. S. Tober, C. F. Larsen, and J. W. Holt. 2024. Surficial geology and proglacial lake change at Sít' Tlein (Malaspina Glacier), Wrangell-St. Elias National Park and Preserve, Alaska. Natural Resource Report NPS/WRST/NRR—2024/2620. National Park Service, Fort Collins, Colorado. https://doi.org/10.36967/2301689

NPS 190/192381, January 2024

Contents

Figures

Tables

Geographic Nomenclature

Sít' Tlein is the traditional Tlingit name for a feature that is located on the traditional lands of the Yakutat Tlingit people but identified officially in the Geographic Names Information System (GNIS)[1] as Malaspina Glacier. In this report and associated map, we consistently use the traditional name, which is documented in GNIS as a variant name for the feature based on ethnographic research. As described in this report, aspects of the foreland of Sít' Tlein are undergoing rapid changes including the development of new lakes that have not been documented in GNIS and, to our knowledge, do not have traditional Tlingit names. For the purposes of this report and the accompanying map, we have adopted unofficial names for two of the largest new lakes. We refer to these as "Sitkagi Lagoon," based on the official name of the associated Sitkagi Bluffs, and "Backdoor Lake." We also apply an unofficial name "Central Zone" to the area encompassing Sitkagi Lagoon and Backdoor Lake where we conducted intensive field sampling. All other geographic names found in this report and the accompanying map are official names documented in GNIS.

[1] https://www.usgs.gov/tools/geographic-names-information-system-gnis

Abstract

Sít' Tlein (Tlingit for "Big Glacier") is the traditional name for what has recently been called Malaspina Glacier, the largest glacier in Alaska. The piedmont terminal lobe of Sít' Tlein is protected from the adjacent Pacific Ocean by a narrow, vegetated foreland dotted with proglacial lakes. Ice of the piedmont lobe is largely covered with debris and vegetation. These lakes and sedimentary deposits impact rates of melt and calving and therefore impact ongoing evolution of the glacier itself. To document these features, we present 1) a new surficial geology map for the foreland and piedmont lobe of Sít' Tlein (an area of 3477 km^2) at a scale of 1:24,000, and 2) a detailed time-series of proglacial lake extents. The surficial geology is referenced to a 2012 IFSAR Digital Terrain Model with 5-m resolution, supplemented with additional satellite images, maps, and digital elevation models. We visited the foreland in 2021 to ground-truth portions of the mapped area. Lake outlines were digitized from Landsat imagery, focusing on lakes adjacent to the central "Seward Lobe" of Sít' Tlein. A majority of the mapping area is occupied by glacier ice, a sizable fraction of which is covered by supraglacial debris of varying thicknesses. Off glacier, in the foreland, glacial outwash is the most common mapping unit, followed by moraines of varying ages and finally by marine beaches, bars, and lagoons. Perhaps surprisingly, given significant changes in the glacier itself over the last half-century, these deposits have not changed dramatically since a similar map was produced by Plafker and Miller in 1958. The most significant changes we found are related to lake development. Other than Malaspina Lake, the largest and most persistent lake in the foreland, proglacial lakes were uncommon in the foreland in 1958. Our mapping shows that lake numbers on the Seward Lobe increased from 5 to more than 200 between 1972 and 2020. Most of the new thermokarst lakes are small, compared to Malaspina Lake, but may be having strong impacts on the future evolution of Sít' Tlein. One of these new lakes, Sitkagi Lagoon, is ice-walled and receives input from the Pacific Ocean, portending the possible initiation of catastrophic tidewater glacier retreat. The full-size digital map (pdf) and GIS data files associated with this report are available at https://irma.nps.gov/DataStore/Reference/Profile/2301821.

Acknowledgments

This project benefited from the support and consultation of NPS colleagues C. Hults, A. Lanik, J. Kenworthy, and C. Scheland. Our understanding of the vast and barely accessible glacier foreland would not be what it is without the guidance and companionship of those with whom we spent time in the field: M. Christoffersen, V. Devaux-Chupin, S. Harper, T. Jones, T. Kuehn, S. Scoggin, M. Truffer, and N. Wagner. Thanks also to colleagues D. Brinkerhoff, K. Timm, and M. Fahnestock for their helpful conversations. We acknowledge the helpful reviews of B. Cellarius, B. Gaglioti, M. Miller, and G. Stock.

We are grateful for the institutions and funding that supported this project. A.C.T. completed this while serving as a Guest Scientist in the Scientist-in-the-Parks Program. Funding for the overall project, and for A.C.T., and for M.G.L. specifically, was provided by the NPS Geological Resources Division and by PMIS project # 230360, “Characterize landscape and park loss from retreat of globally significant Malaspina Glacier.” S.A.M., B.S.T., and J.W.H. were supported by National Science Foundation award 1929577, and B.S.T. also by NASA FINESST award 80NSSC19K1357. C.F.L. was supported by Operation IceBridge Alaska, award NNX16AC32G and National Science Foundation award 1929566.

Introduction

Sít' Tlein ("Big Glacier") is a traditional, and apt, Tlingit name for what has only recently been called Malaspina Glacier (Thornton 2012). Sít' Tlein is the largest glacier in Alaska and is part of the 3rd largest glacier complex in the world (Windnagel et al. 2022). Changes in the geometry, dynamics, and terminus configuration of Sít' Tlein are therefore of great interest to local residents (including members of the Yakutat Tlingit Tribe); to glaciologists, ecologists, and oceanographers; and to managers of the two protected areas that span the glacier's length from its headwaters (Canada's Kluane National Park) to its terminus (Wrangell-St. Elias National Park and Preserve).

Here, we present a map of the surficial geology of the piedmont lobe of Sít' Tlein, including the glacier forelands that skirt its broad fan-shaped terminus for a distance of over 100 km between Point Riou (to the west, at the margin of Icy Bay) and Blizhni Point (to the east, at the margin of Yakutat Bay). We focus on this area—which excludes higher elevation and perennially snow-covered portions of the glacier (Figure 1)—because it is the zone where glacier change typically occurs most rapidly. It is also the area where geomorphic and hydrologic changes, such as the development and evolution of proglacial lakes and rivers, have the potential to rapidly destabilize the glacier margin. To emphasize the importance of rapid hydrologic change, this report includes separate maps of the temporal evolution of lakes on and around the glacier terminus since 1972.

The piedmont lobe of Sít' Tlein receives ice flow from three primary upstream basins: the Agassiz, Seward, and Marvine. Collectively, the glacier ice of Sít' Tlein covers 4640 km^2 (based on the Randolph Glacier Inventory 6.0; Pfeffer et al. 2016), and the area mapped for this project—which excludes much of the upstream accumulation area but includes the off-glacier portion of the glacier foreland as described above, covers 3477 km^2.

This project was initially conceived, in part, as a follow-up to surficial mapping done by George Plafker and Don Miller (1958). That project mapped a comparable portion of Sít' Tlein, and similarly focused on both the glacier foreland and the glacier ablation zone. Given that the 1958 publication was based upon interpretation of aerial photographs collected in 1948, the present work provides an opportunity to assess well over a half-century of change. Observations of Sít' Tlein date back even further in time. Plafker and Miller's 1958 report provides a useful overview of earlier scientific investigations, dating back to Israel Russell's 1890 expedition (Russell 1891). Russell's article summarizes even earlier expeditions that contributed to western understanding of the area's broad character and geography starting with Vitus Bering's expedition of 1741, and including later visits by La Perouse, in 1786, and by Tebenkov, who mapped the Sít' Tlein coastline in 1847 (Tebenkov 1852). We note here that all these efforts were predated by the deep knowledge of this landscape by indigenous people including—at various times—members of the Eyak, Tlingit, and Athapaskan nations. Their explorations have been recorded primarily through the oral tradition, as summarized (with particular emphasis on this glacial landscape) by Cruikshank (2001).

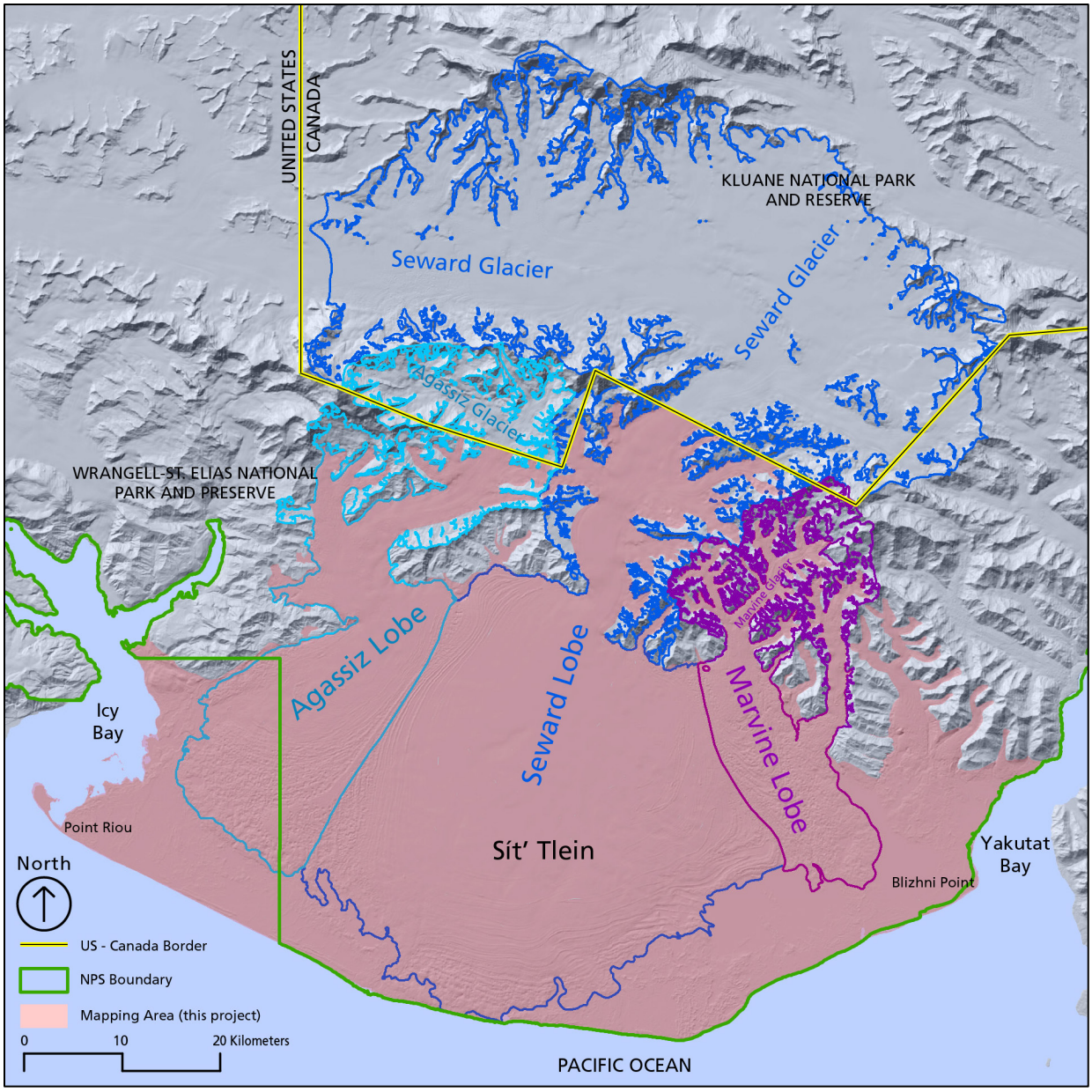

Figure 1. Broad landscape context for Sít' Tlein, showing area mapped in this project (highlighted in transparent red). The piedmont portion of Sít' Tlein is fed by coalesced ice lobes from three glaciers, Agassiz, Seward, and Marvine Glaciers.

A wide variety of scientists have worked in and around Sít' Tlein since Plafker and Miller's 1958 map, and we briefly summarize only the most relevant of those efforts here. Roughly coincident with Plafker and Miller's work, Robert P. Sharp published three works reporting on extensive fieldwork there over the prior decade studying mass balance (1951), terminus fluctuations (1958a), and the overall glacier dynamics (1958b). Bedrock geology of the area was covered by Miller (1961) and later by Richter et al. (2006) in addition to numerous statewide and regional compilation maps. Gustavson (1974, 1975a, 1975b) made multiple visits to Malaspina Lake and the surrounding portions of the foreland, focusing largely on hydrology and sedimentation. Muskett et al. (2003,

2008) and Sauber (2005) conducted early remote sensing-based investigations of mass change and patterns of thinning at Sít' Tlein. Muskett et al. (2008) provided particularly good information about the pattern of the 1986–87 surge. Subsequent studies of thinning patterns used the satellite-borne GRACE mission (Luthcke et al. 2008) and airborne lidar (Loso et al. 2014, Larsen et al. 2015). Larsen et al. (2005) summarized the impacts of long and short-term glacier thinning on isostatic uplift, with direct impact on coastal topography. Sparse radar soundings combined with surface velocities and ice topography were used by Ford et al. (2003), Conway et al. (2009), Rignot et al. (2013), and Cotton et al. (2014) to infer the nature and tectonic structure of the glacier's bed. Barclay et al. (2001, 2006), Elmore et al. (2013), Zurbuchen et al. (2015), and Gaglioti et al. (2019) all produced works bearing on the historic pattern of glacier expansion and retreat by Sít' Tlein and its adjacent glacier neighbors. The specific relevance of debris and vegetation cover on glaciers, including Sít' Tlein, was addressed by Fickert et al. (2007, 2022). New work by Tober et al. (2023) uses airborne radar soundings to estimate the thickness of Sít' Tlein ice and the topography of the glacier bed.

Objectives

Since the time of the Plafker and Miller (1958) map, some aspects of the Sít' Tlein foreland have obviously changed rapidly. Most conspicuous has been the growth of new proglacial lakes that simply did not exist in the 1950s (see the photograph on the cover of this report). In other ways, however, it seems that the terminus area has been remarkably stable for the last half century. The ice margin, for example, has with only a few exceptions (adjacent to the proglacial lakes) barely retreated. This is in marked contrast to the nearly ubiquitous and sometimes dramatic retreat of literally thousands of glacier termini around Alaska (e.g., Loso et al. 2014). Most fundamentally, the objective of this project is to understand this apparent contradiction: in what ways have the ice margin and the landforms of the Sít' Tlein piedmont lobe changed since 1958, and to what extent? Of course, there are many ways to measure change, and this project focuses on just one: the spatial distribution of ice, water, and sedimentary cover in and around the glacier margin. To do so, this project does the following:

- Use the Pacific Ocean (to the south) and the line of bedrock exposures on the northern foothills to bound the study area, thus including the ice and debris cover of the piedmont lobe as illustrated in Figure 1;
- Map at 1:24,000 the boundaries of terrestrial surficial sedimentary units throughout the study area for a single point in time (summer 2012);
- Describe the character and to the extent possible, the age and origin, of those deposits;
- Supplement the static map with detailed maps of the temporal evolution of proglacial lakes from 1972 to 2020; and
- Using these products, assess the nature and implications of recent and ongoing changes to the Sít' Tlein foreland.

Methods

This mapping project consists of two discrete products. The first is a static surficial geology map of the entire Sít' Tlein piedmont lobe. The second is a time-series of proglacial lake outlines evolving between 1972 and 2020. We describe the methods and data sources for these two products in order. As described earlier, both products are bounded by an overall project outline defined by the Pacific Ocean to the south, Icy Bay and Yakutat Bay to the west and east respectively, and the foot of the first range of foothills bounding the piedmont lobe to the north. The mapping area mostly lies between sea level and about 500 m but reaches over 1700 m at the head of the Marvine Glacier, southwest of Mt. Cook. We do not include the much higher upper accumulation zone of the Seward Lobe.

Static Surficial Geology Map

Because the entire mapping area is so dynamic, we chose a master data source and corresponding reference date for the entire map. Surficial geology units were mapped in reference to a 2012 Interferometric Synthetic Aperture Radar (IFSAR) derived Digital Terrain Model (DTM—bare ground elevations with the first returns [vegetation—where applicable—filtered out]). This 5-meter DTM was collected with an acquisition date range of August 14 to September 8, 2012 (Fugro EarthData 2016). A hillshade version of this map was selected as the primary reference because it is publicly available, it provides complete coverage of the study area, and its horizontal resolution and accuracy are high enough to provide crisp and precise evidence of unit contacts at the nominal 1:24,000 mapping scale.

We supplemented the IFSAR dataset with a broad variety of data sources to help us interpret, describe, and confirm the mapping units. A lidar-based 1-meter resolution DTM collected in June 2020 was very helpful in seeing details under dense vegetation, but its coverage was limited to the central portion of the glacier forelands roughly between Malaspina Lake and Fountain Stream. In some areas we compared that DTM with other, mostly older DTMs in search of evidence for ground subsidence that would point towards the presence of buried glacier ice. We were unable to find good quality cloudless optical imagery from 2012, but Landsat imagery from 2013 and 2014 and 2016 Sentinel-2 imagery were very helpful in distinguishing and describing more vegetated portions of the map. In the case of disparity between IFSAR and supplementary data, preference was given to the IFSAR dataset to maintain a consistent reference date.

The IFSAR DTM was an unreliable source in only a few settings. The shoreline boundary between coastal beaches and the ocean was not well defined on the IFSAR DTM, possibly because of tidal variations over the multiple days of acquisition. Instead, the shoreline was mapped with greater reliance on 2016 Sentinel imagery between Taan Fjord and Gull Island, 2014 Landsat imagery between Gull Island and Yahtse River, 2013 Landsat imagery between Yahtse River and Sudden Stream, and 2016 Sentinel imagery between Sudden Stream and Yakutat Bay. Thinner layers of supraglacial debris on the piedmont portion of the glacier were not evident in the DTM (insufficient to cause significant differential melting and hence generating little topographic signature) and were instead mapped from 2013 Landsat imagery supplemented in a few areas by 2014 Landsat imagery.

Identification of the modern (nominally 2012) ice margin was made difficult by the presence of both supraglacial debris and, in most cases, extensive vegetation growth. The ice margin was identified by abrupt changes in ground texture, context within the landscape, and especially by the presence of thermokarst. For this sometimes-challenging contact, we relied more than usual on additional data sources, including the 2020 lidar, other digital elevation models (to detect thaw-induced ground subsidence) and all available sources of historic imagery. The slow pace of melt and terminus retreat under heavy vegetation allowed us to rely on these data sources from other time periods without significantly biasing our results. We note some remaining uncertainty about the location of modern ice margin immediately west of Malaspina Lake, between it and Manby Stream.

Historic ice extents, the vegetation margin, and flowlines were mapped using a variety of sources. Evidence of the 1986–87 surge, which affected only the eastern portion of the piedmont lobe, was captured well and mapped from Landsat and other satellite imagery sources. The boundaries of older historic ice extents were drawn with reference to the Plafker and Miller map (1958). We generally accepted their inferred historic glacier boundaries, with slight adjustments to align more precisely with their respective morainal deposits visible in the modern, more detailed imagery. The vegetation boundary was drawn with reference to 2013 Landsat imagery to reflect the most upstream (northward) extent of vegetation cover on the glacier surface. The most downstream (southward) extent of vegetation is in almost all cases coincident with the beach margin and was not mapped as a distinct contact. Mapped flowlines trace parallel linear ridges and depressions in the foreland but are not comprehensive. Indicated directionality is based on the inference that these linear features reflect former ice flow paths.

The mapping units used in this project (Table 1) describe all surfaces within the mapping area. Because bedrock exposures in the foothills were explicitly omitted from the mapping area, no bedrock units are included. Glacier ice is treated as a mapping unit subdivided on the basis of debris cover quantity and type as visible on 2013 Landsat imagery. Lake boundaries (mostly for proglacial lakes but also including some supraglacial lakes and broad active river channels; no effort was made to map most narrow river channels) were mapped from distinctive flat areas on the IFSAR DTM. The remaining areas are all surficial deposits, exclusively Quaternary in age, that are classified in a manner simplified from Plafker and Miller (1958). Morainal deposits were identified and distinguished by the presence and direction of flowlines and moraines. Outwash deposits were identified by floodplain topography and distinguished based on stream activity and vegetation. Beach and bar deposits were identified on the basis of location and morphology and subdivided on the basis of vegetation cover.

Table 1. Mapping units and brief descriptions. Comparable mapping units in the Plafker and Miller (1958) map are listed; differences are noted in the text.

Unit Code	Unit Name	Unit Description	Plafker correlate
w	Water	Impounded or flowing freshwater, including proglacial and supraglacial lakes and also active river channels greater than ~15 m width.	None [A]
Qi	Clean Ice	Glacier ice free of, or minimally covered by, surficial debris. White or very light gray in appearance.	None [A]
Qdms	Minor Supraglacial Debris	Thin and/or discontinuous medial moraines and debris on the glacier surface; light in color and typically only one to several clasts thick with ice or moisture from melt visible at the surface.	None [B]
Qdts	Thick Supraglacial Debris	Thick and/or continuous medial moraines and debris on the glacier surface; dark in color and typically with no ice visible among the clasts.	None [B]
Qos	Supraglacial Outwash	Debris on the glacier surface that has been transported, sorted, and deposited by supraglacial streams.	None [B]
Qm2	Younger End and Ground Moraine	Surface gently undulating, largely covered with brush and scattered trees. Arrows are drawn along axes of elongate ridges and depressions to indicate inferred direction of ice movement.	Qym
Qm1	Older End and Ground Moraine	Surface hummocky, largely covered with mature forest. Arrows are drawn along axes of elongate ridges and depressions to indicate inferred direction of ice movement.	Qom
Qmu	Undifferentiated Moraine	Interlobate and lateral moraine deposits of uncertain age along mountain front; covered with brush and trees.	Qum
Qo2	Younger Outwash	Deposits of existing glacial streams, including active braidplains and floodplains; thin active channels not necessarily shown or mapped. Largely bare of vegetation.	Qo
Qo1	Older Outwash	Deposits of former glacial streams, largely vegetated with brush and/or forest. Single channel streams may still be present.	Qco
Qb2	Younger Marine Beach, Bar, and Spit Deposits	Comparatively recent unvegetated beach deposits.	Qmy
Qb1	Older Marine Beach, Bar, and Spit Deposits	Beach deposits with brush and trees.	Qmi, Qmo
Qbu	Marine Beach, Bar, and Lagoon Deposits, Undifferentiated	Linear beach and bar deposits covered with brush and trees, alternating with flat wet areas with little vegetation.	Qml, Ql

[A] Plafker and Miller mapped water and glacier ice but did not designate them as formal mapping units.

[B] Plafker and Miller mapped supraglacial debris but did not designate it as a formal mapping unit, and did not distinguish among debris quantities (minor, thick) or qualities (outwash).

Most of our mapped surficial deposit units have a direct correlation in the 1958 Plafker and Miller map (Table 1), with a few exceptions. We combined all well-vegetated marine beach, bar, and spit deposits into our Qb1, while Plafker and Miller differentiated the unit by age, basing their inferences on vegetation cover. For them, units covered by brush/trees were Qmi, and those covered with mature forest were Qmo. Plafker and Miller also had a unique mapping unit for wet unvegetated marine lagoons (their Ql). We found that at the 1:24,000 mapping scale these could not be consistently distinguished from better drained marine beaches, bars, and spits mantled by vegetation that varied with age. We therefore included marine lagoons in our Qbu (marine beach, bar, and lagoon deposits, undifferentiated) unit. Similarly, Plafker and Miller had a unique mapping unit for poorly vegetated wetlands that were less clearly associated with coastal landforms (their Qll). We found this unit to be more reflective of hydrologic condition (periodic soil saturation that inhibits growth of woody vegetation) than of a surficial deposit type, so we omitted this mapping unit and instead categorized poorly vegetated wet areas according to the inferred underlying deposit. We also did not identify or map any deposits correlated directly with Plafker and Miller's units Qoo (Channeled outwash from the Yakutat Bay Lobe), Qye (Esker Deposits), or Qd (Dune Deposits).

The mapped surficial geology units were not explicitly or consistently ground-truthed, but we did visit portions of the mapping area in summer 2021. Over the course of that summer, we visited portions of the glacier foreland roughly between Fountain Stream and Sudden Stream while focused on research tasks related to, but distinct from, this project. Most of our ground-based work was on or adjacent to the larger proglacial lakes, but we were able to view a larger portion of the area during repeated low aerial overflights by helicopter. The final mapping presented here was influenced and improved by those site visits, but this map should nonetheless be viewed primarily as an interpretation of remote sensing data.

Proglacial Lake Outlines

Over the course of this project, we recognized that rapid and consequential changes in the sizes, locations, and shapes of lakes within the mapping area deserved special attention. We generally refer to these collectively as 'proglacial lakes' although there are some minor supraglacial lakes as well. Our initial intent was to map the evolving lake outlines as annotated features on the main surficial geology map, but the lake evolution was ultimately too complicated to show clearly on a single map. We therefore map and display the evolving lake boundaries separately from the rest of the features within our mapping area, reiterating that the static surficial geology map depicts lake boundaries referenced specifically to the moment depicted by the 2012 IFSAR DTM.

The time-series of lake outlines was manually digitized from publicly available Landsat imagery. We selected a single cloud-free melt season (April–October) image for each year from 1972–2020 and then traced the boundaries of all visible impounded surface water from a subset of those images. We often needed more than one scene to obtain cloud-free coverage of the entire study area; scenes used in this project are listed in Table 2. The base images were all viewed as true-color 30 m tiffs for consistency among years. Minimum theoretically detectable lake size was therefore 0.001 km^2 (1 pixel) and that is the size of the smallest digitized lake in our dataset, but the population-wide mean digitized lake size was almost three orders of magnitude larger (0.786 km^2). Imagery quality did

generally increase over the course of the 1972–2020 period, and in particular the spatial resolution of the earliest Landsat sensors was 60 m (larger than our mapping resolution) until around 1982. Other uncontrolled parameters like lighting and clouds varied randomly in ways that contribute noise to the final time series. Notably, seasonal variations in hydrologic conditions caused lake sizes to fluctuate.

Lake outlines were digitized downstream of Seward Lobe (we excluded lakes downstream of the Agassiz and Marvine lobes). Years selected for digitizing varied by area (Table 3). Over most of the Seward Lobe, we digitized boundaries roughly every 5 years until 2010, and with increased frequency until 2020. In the Central Zone (Figure 2 and Table 3), we enhanced temporal resolution by measuring every year, if possible, beginning in 1972. Specific years included in the dataset were constrained by availability of complete, good quality, cloud free images. In total, from 1972–2020, we digitized 16 years of boundaries for the entire study area and 36 years in the Central Zone.

Table 2. Landsat scenes used for proglacial lake outlines. In years with more than one scene, spatial overlaps were resolved in favor of the last listed scene.

Year	Landsat Scene Name
1972	LM01_L1TP_063018_19720811_20180428_01_T2
1973	LM01_L1TP_062018_19730910_20180428_01_T2
	LM01_L1TP_063018_19730911_20180428_01_T2
1974	LM01_L1TP_063018_19740906_20180427_01_T2
1975	LM01_L1TP_062018_19750813_20180426_01_T2
	LM01_L1TP_063018_19750814_20180426_01_T2
1976	LM02_L1TP_062018_19760816_20180424_01_T2
1977	LM02_L1TP_063018_19770707_20180422_01_T2
1978	LM03_L1TP_062018_19780622_20180420_01_T2
	LM03_L1TP_063018_19780729_20180421_01_T2
1979	LM02_L1TP_062018_19790819_20180419_01_T2
	LM02_L1TP_063018_19790820_20180419_01_T2
1980	LM02_L1TP_063018_19800709_20180416_01_T2
1981	LM02_L1TP_063018_19810722_20180415_01_T2
	LM02_L1TP_062018_19810808_20180415_01_T2
1982	LM04_L1TP_063018_19820814_20180413_01_T2
	LM04_L1TP_062018_19820924_20180414_01_T2
1983	LM04_L1TP_063018_19830902_20180412_01_T2
	LM04_L1TP_062018_19830911_20180412_01_T2

Table 2 (continued). Landsat scenes used for proglacial lake outlines. In years with more than one scene, spatial overlaps were resolved in favor of the last listed scene.

Year	Landsat Scene Name
1984	LM05_L1TP_062018_19840921_20180410_01_T2
	LT05_L1TP_063018_19840912_20161004_01_T1
1985	LM05_L1TP_063018_19850830_20180407_01_T2
	LT05_L1TP_061018_19850715_20161004_01_T1
	LM05_L1TP_062018_19850807_20180407_01_T2
1986	LT05_L1TP_063018_19860918_20161003_01_T1
	LT05_L1TP_062018_19860911_20161003_01_T1
1987	LT05_L1TP_062018_19870829_20161002_01_T1
	LT05_L1TP_061018_19870822_20161002_01_T1
1988	LT04_L1TP_063018_19880627_20161003_01_T1
	LT04_L1GS_062018_19880823_20161002_01_T2
	LT05_L1TP_061018_19880909_20161002_01_T1
1989	LM05_L1TP_061018_19890827_20180325_01_T2
1990	LT05_L1TP_062018_19900720_20161002_01_T1
	LT05_L1TP_063018_19900812_20161002_01_T1
1991	LT05_L1TP_063018_19910714_20160929_01_T1
	LT05_L1TP_061018_19910614_20160930_01_T1
	LT05_L1TP_062018_19910621_20160929_01_T1
1992	LT05_L1TP_063018_19920817_20160929_01_T1
	LT05_L1TP_062018_19920810_20160929_01_T1
	LT05_L1TP_061018_19920904_20160928_01_T1
1993	LT05_L1TP_063018_19930905_20160927_01_T1
	LT05_L1TP_062018_19930712_20160928_01_T1
1994	LT05_L1TP_061018_19940809_20160927_01_T1
	LT05_L1TP_062018_19940816_20160927_01_T1
1995	LT05_L1TP_061018_19951015_20160925_01_T1
	LT05_L1TP_062018_19950904_20160926_01_T1
	LT05_L1TP_063018_19950709_20160926_01_T1
1996	LT05_L1TP_061018_19960814_20160925_01_T1
	LT05_L1TP_062018_19960906_20160924_01_T1

Table 2 (continued). Landsat scenes used for proglacial lake outlines. In years with more than one scene, spatial overlaps were resolved in favor of the last listed scene.

Year	Landsat Scene Name
1997	LT05_L1TP_062018_19971011_20160925_01_T1
	LT05_L1TP_061018_19970630_20160925_01_T1
	LT05_L1TP_063018_19970916_20160923_01_T1
1998	LT05_L1TP_062018_19980928_20160923_01_T1
	LT05_L1TP_061018_19980804_20160923_01_T1
1999	LT05_L1TP_062018_19990713_20160919_01_T1
	LE07_L1TP_061018_19990714_20161003_01_T1
	LE07_L1TP_063018_19990728_20161003_01_T1
2000	LE07_L1TP_062018_20000909_20161001_01_T1
	LE07_L1TP_063018_20000831_20161001_01_T1
2001	LE07_L1TP_062018_20010624_20161001_01_T1
	LE07_L1TP_063018_20010903_20161001_01_T1
	LE07_L1TP_061018_20010921_20160929_01_T1
2002	LE07_L1TP_062018_20020713_20160929_01_T1
	LE07_L1TP_063018_20020805_20160928_01_T1
2003	LT05_L1TP_061018_20031021_20160915_01_T1
	LT05_L1TP_062018_20030809_20160915_01_T1
2004	LE07_L1TP_061018_20041015_20160926_01_T1
	LE07_L1TP_062018_20040803_20160926_01_T1
2005	LT05_L1TP_062018_20050814_20160912_01_T1
	LT05_L1TP_061018_20050908_20160912_01_T1
2006	LT05_L1TP_062018_20060801_20160910_01_T1
	LT05_L1TP_063018_20060925_20160911_01_T1
2007	LT05_L1TP_062018_20070719_20160907_01_T1
	LT05_L1TP_063018_20070811_20160908_01_T1
2008	LT05_L1TP_061018_20080831_20160905_01_T1
	LT05_L1TP_062018_20080705_20160906_01_T1
	LT05_L1TP_063018_20080728_20160905_01_T1
2009	LT05_L1TP_062018_20090708_20160904_01_T1
	LT05_L1TP_061018_20090717_20160904_01_T1

Table 2 (continued). Landsat scenes used for proglacial lake outlines. In years with more than one scene, spatial overlaps were resolved in favor of the last listed scene.

Year	Landsat Scene Name
2010	LT05_L1TP_061018_20100922_20160901_01_T1
	LT05_L1TP_062018_20100913_20160901_01_T1
	LT05_L1TP_063018_20100920_20160831_01_T1
2011	LT05_L1TP_062018_20110527_20160901_01_T1
	LT05_L1TP_061018_20110723_20160831_01_T1
	LT05_L1TP_063018_20110806_20160831_01_T1
2012	LE07_L1TP_061018_20120818_20160910_01_T1
	LE07_L1TP_062018_20121012_20160909_01_T1
2013	LC08_L1TP_062018_20131007_20170308_01_T1
	LC08_L1TP_063018_20130811_20170309_01_T1
	LC08_L1TP_061018_20130813_20170309_01_T1
2014	LC08_L1TP_062018_20140823_20170303_01_T1
	LC08_L1TP_061018_20140731_20170304_01_T1
2015	LC08_L1TP_062018_20150623_20170226_01_T1
	LC08_L1TP_063018_20150614_20170226_01_T1
	LC08_L1TP_061018_20150803_20170226_01_T1
2016	LC08_L1TP_062018_20160828_20170221_01_T1
	LC08_L1TP_063018_20161006_20170220_01_T1
	LC08_L1TP_061018_20161008_20170220_01_T1
2017	LC08_L1TP_061018_20170808_20170823_01_T1
	LC08_L1TP_062018_20170815_20170825_01_T1
	LC08_L1TP_063018_20170806_20170813_01_T1
2018	LC08_L1TP_063018_20180910_20180927_01_T1
	LC08_L1TP_062018_20180919_20180928_01_T1
2019	LC08_L1TP_063018_20190828_20190903_01_T1
	LC08_L1TP_062018_20190906_20190917_01_T1
	LC08_L1TP_061018_20190830_20190916_01_T1
2020	LC08_L1TP_061018_20200715_20200715_01_T1
	LC08_L1TP_063018_20200729_20200807_01_T1

Table 2 (continued). Landsat scenes used for proglacial lake outlines. In years with more than one scene, spatial overlaps were resolved in favor of the last listed scene.

Year	Landsat Scene Name
2021	LC08_L1TP_061018_20210718_20210729_01_T1
	LC08_L1TP_063018_20210716_20210729_01_T1

Table 3. Years in which lake boundaries were digitized for the entire Seward Lobe or for only a subset of that area in the Central Zone. 'x' indicates mapping was completed.

Year	Seward Lobe	Central Zone	Note
1972	x	x	–
1973	–	x	–
1974	–	–	No cloud free images
1975	x	x	–
1976	–	–	No cloud free images
1977	–	x	–
1978	–	–	No cloud free images
1979	–	x	–
1980	x	x	–
1981	–	x	–
1982	–	x	–
1983	–	x	–
1984	–	x	–
1985	–	–	No cloud free images
1986	x	x	–
1987	–	x	–
1988	–	x	–
1989	–	–	Quality & projection issues
1990	x	x	–
1991	–	x	–
1992	–	x	–
1993	–	x	–
1994	–	–	No cloud free images

Table 3 (continued). Years in which lake boundaries were digitized for the entire Seward Lobe or for only a subset of that area in the Central Zone. ‘x’ indicates mapping was completed.

Year	Seward Lobe	Central Zone	Note
1995	–	–	No cloud free images
1996	x	x	–
1997	–	x	–
1998	–	x	–
1999	–	x	–
2000	x	x	–
2001	–	–	No cloud free images
2002	–	x	–
2003	–	x	–
2004	–	x	–
2005	x	x	–
2006	–	–	No cloud free images
2007	–	x	–
2008	–	–	No cloud free images
2009	–	x	–
2010	x	x	–
2011	–	–	No cloud free images
2012	–	–	No cloud free images
2013	x	x	–
2014	x	x	–
2015	x	x	–
2016	x	x	–
2017	–	–	No cloud free images
2018	x	x	–
2019	x	x	–
2020	x	x	–

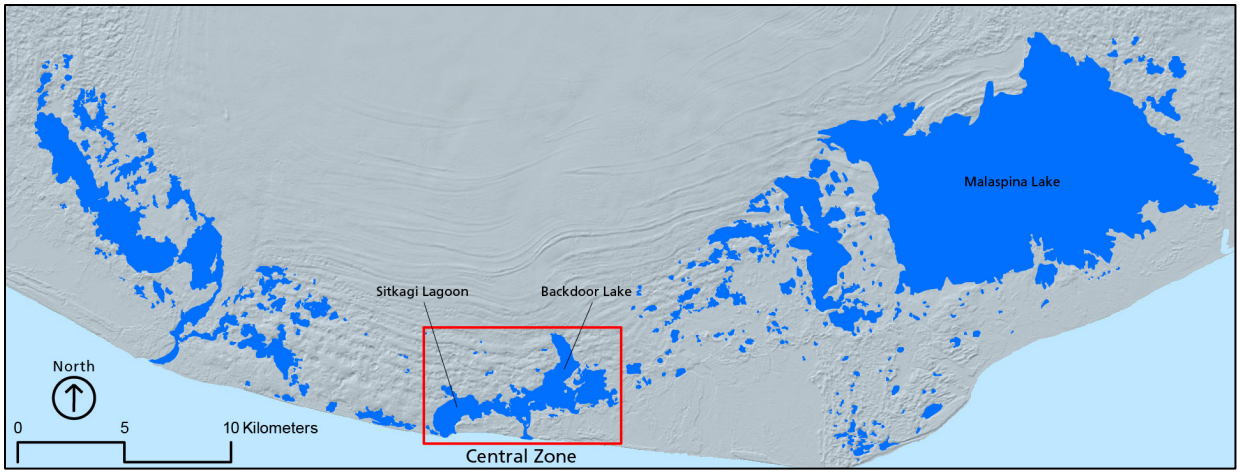

Figure 2. Lakes digitized during this project along the Seward Lobe foreland, aggregated across all years (blue polygons). The red rectangle depicts the Central Zone selected for more temporally intensive sampling, with a focus on Sitkagi Lagoon and Backdoor Lake.

Results and Discussion

Static Surficial Geology Map

The compiled surficial geology map is shown at reduced scale in Figure 3, and the full-sized high-resolution poster version is available at https://irma.nps.gov/DataStore/Reference/Profile/2301821. Vectorized polygon and lineation data suitable for use in geospatial software are archived and available at that same location. Below, we discuss the results of this mapping effort in order of map unit, roughly in descending order of areal coverage (Table 4).

Table 4. Number and areal coverage (in km^2) for units within the mapping area. '% Cover' refers to the portion of the 3477 km^2 mapping area covered by a given unit.

Unit Code	Unit Name	Number	Minimum Area	Maximum Area	Mean Area	Total Area	% Cover
w	Water	1085	0.0014	97.3958	0.1516	164.4937	4.7
Qi	Clean Ice	132	0.0167	327.4368	5.0359	664.7407	19.1
Qdms	Minor Supraglacial Debris	64	0.0185	460.5114	9.3976	601.4488	17.3
Qdts	Thick Supraglacial Debris	77	0.0043	1358.8837	19.0957	1470.3723	42.3
Qos	Supraglacial Outwash	25	0.0051	4.8961	0.7842	19.6039	0.6
Qm2	Younger End and Ground Moraine	88	0.0016	19.9260	1.1225	98.7769	2.8
Qm1	Older End and Ground Moraine	15	0.0045	34.9621	4.7876	71.8135	2.1
Qmu	Undifferentiated Moraine	4	0.9506	5.5041	3.1103	12.4411	0.4
Qo2	Younger Outwash	113	0.0002	42.9110	0.6407	72.3946	2.1
Qo1	Older Outwash	54	0.0000	65.6307	4.3401	234.3675	6.7
Qb2	Younger Marine Beach, Bar, and Spit Deposits	38	0.0014	4.9718	0.5643	21.4449	0.6
Qb1	Older Marine Beach, Bar, and Spit Deposits	12	0.0056	2.5125	0.5401	6.4815	0.2
Qbu	Marine Beach, Bar, and Lagoon Deposits, Undifferentiated	31	0.0272	8.0023	1.2366	38.3346	1.1

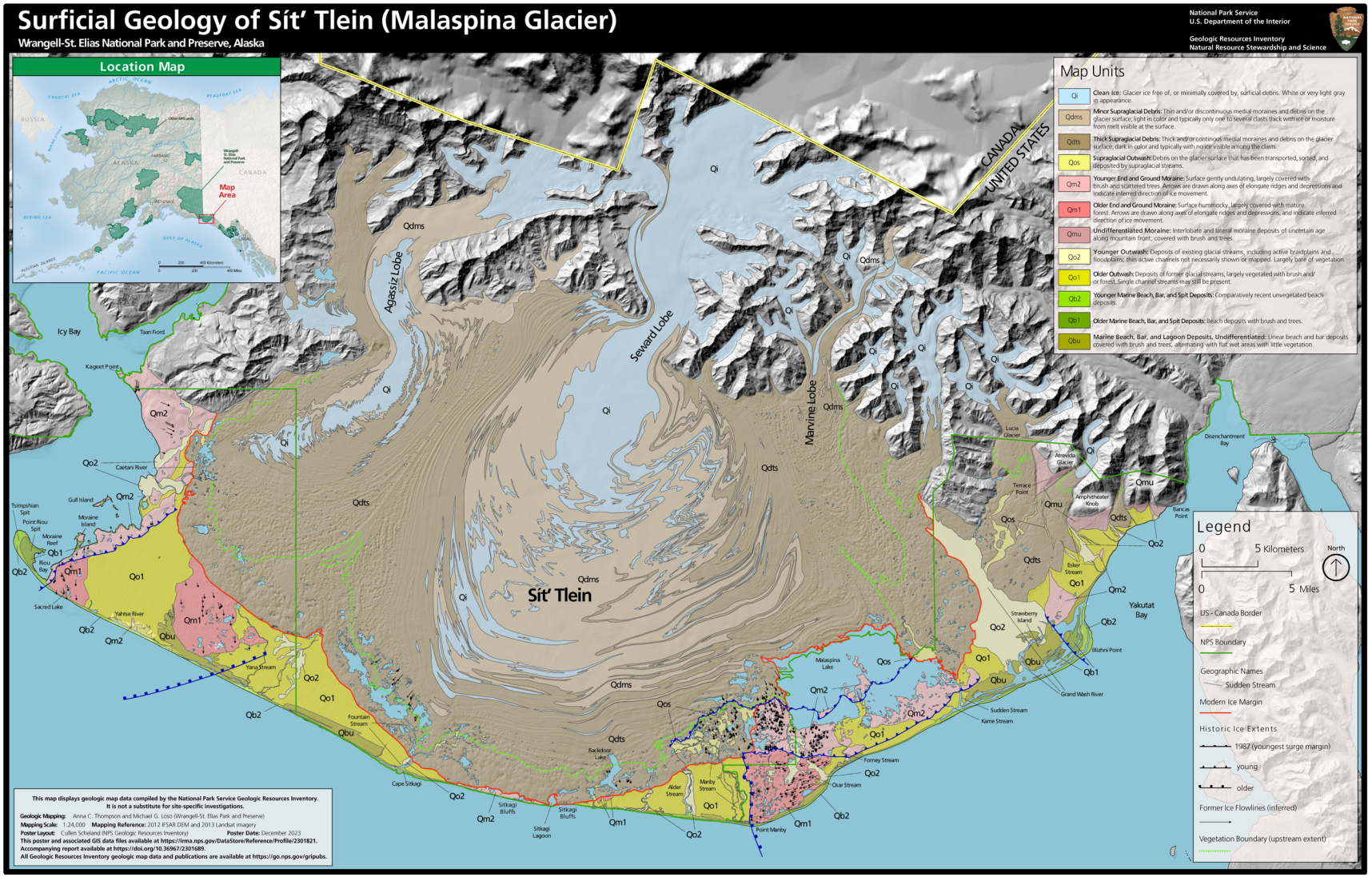

Figure 3. Small-format surficial geologic map of Sít' Tlein. Full-size digital copy available at https://irma.nps.gov/DataStore/Reference/Profile/2301821.

Most of the mapping area is dominated by the ice of the piedmont lobe itself. Glacier ice collectively covers nearly 80% of the mapping area, and well over half of that is debris-covered – mostly with thick supraglacial debris (Qdts). Generally speaking, glacier cover in the area has not changed appreciably since Plafker and Miller's 1958 map. Except in the vicinity of Malaspina Lake, the modern ice boundary we mapped does not vary more than 1 km from the boundary mapped in 1958. Our contemporary ice margin is both more and less advanced than Plafker and Miller's, depending on location along the foreland, suggesting that most of these relatively small differences are more attributable to mapping errors than actual marginal retreat. The difficulty of identifying the ice margin under thick vegetated debris supports this interpretation, and we note that our mapping efforts were aided significantly by the ability to compare sequential digital elevation models for evidence of ground subsidence presumably caused by the melt of buried ice—a source of information unavailable to Plafker and Miller.

In the vicinity of Malaspina Lake, the more substantial change (retreat) of the ice margin can be attributed to the substantial growth of Malaspina Lake since 1958. Numerous other lakes have also appeared or grown since Plafker and Miller's project, and collectively these contribute to the importance of water (w) as the second most dominant mapping unit with almost 5% coverage of the mapping area at the time of the IFSAR DTM. As noted previously, some of the lakes are not technically proglacial. They lie within the glacier margin and are hence more appropriately termed supraglacial. These generally occur within areas of substantial thermokarst development and are often ringed by steep debris-covered ice cliffs mantled by alders and sometimes other vegetation. In any case, the collective amount of impounded water along the glacier foreland is large and substantially growing, as documented later in this report.

Outwash from glacial streams is the next most common mapping unit and is mostly found in front of the modern ice margin. Younger outwash (Qo2) is mostly found in association with contemporary glacial river outlets of the piedmont lobe, including Esker Stream, Grand Wash River, Osar Stream, Alder Stream, Fountain Stream, Yana Stream, and the Caetani River. Older outwash (Qo1), distinguished by heavier vegetation cover, is much more widespread and reflects the ephemeral nature of glacial streams in the foreland. As with most glacial rivers, individual channels in Sít' Tlein's foreland are prone to lateral migration that allows the development of vegetation on older braids. But more important to the dominance of older outwash in this setting is the abrupt abandonment of entire rivers, which has occurred repeatedly throughout the foreland. The most notable example is the abandonment of Yahtse River, which was formed in the western foreland by outwash from the advanced lobe of Yahtse Glacier from neighboring Icy Bay. Yahtse Glacier retreated in the late 19th century, leaving the outwash delta largely free of ongoing fluvial activity (Plafker and Miller 1958, Barclay et al. 2006). Another minor contributor to the importance of older outwash, in comparison with the Plafker and Miller (1958) map, is the development of vegetation in the interval between the two mapping efforts. Some of the outwash deposits that were young and comparatively unvegetated at the time of the 1958 mapping have since grown over. A small amount of the third outwash unit was mapped on the surface of the piedmont lobe itself (Qos). Most Qos deposits were near the shores of Malaspina Lake and closely associated with the margin of the 1986–

87 surge. We interpret most of this outwash as having been deposited on thin stagnant glacier ice by rivers emanating from the thickened lobe of the advancing ice during the surge.

Moraines cumulatively cover about 5% of the mapping area. Boundaries between moraines, outwash, and even ice were often difficult to discern in satellite imagery and even on the ground due to the presence of heavy forest cover on portions of all three units. Our ability to draw such distinctions was dependent in many cases on the use of the bare-ground elevation models from the IFSAR and especially from the 2020 lidar-based DTM (Figure 4). Those terrain models allowed us in many cases to draw boundaries more accurately, we suspect, than previous investigators. It also allowed us to infer the flow directions of former advances, which in some cases helped us to distinguish between moraines deposited by the different advances. A good example of this is where WSW-flowing ice from the Hubbard Glacier deposited a moraine to the south of Malaspina Lake, which was subsequently overridden by a younger advance of the Seward Lobe of Sít' Tlein flowing SSE. Younger moraines (Qm2) are the most common and were differentiated from older moraines (Qm1) by the degree of vegetation cover and especially by the presence, on older moraines, of mature forest.

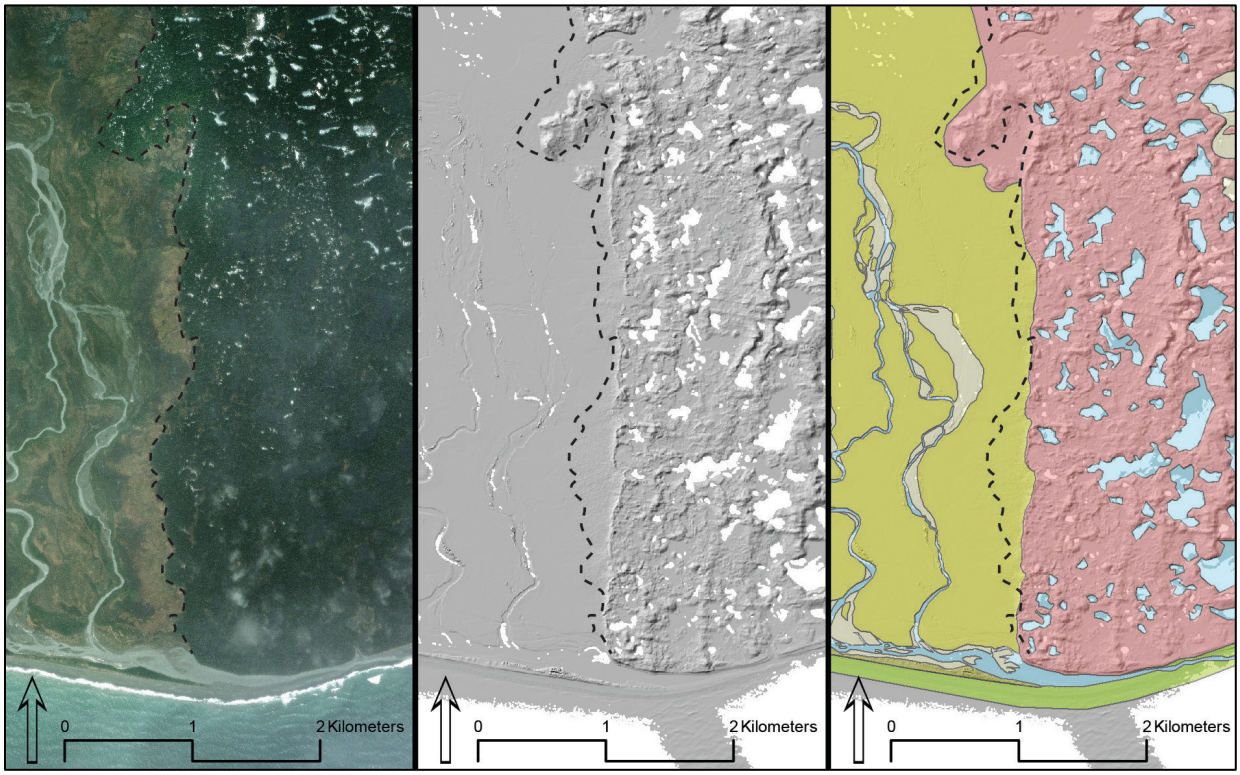

Figure 4. Comparison of area near Point Manby using a satellite image (left) and a lidar-based bare earth hillshade basemap (center). The transparent mapping unit overlying the lidar basemap (right) shows how we were able to trace the outwash/moraine boundaries (yellow/pink polygons) more accurately using the lidar than by following the forest boundary (dashed line in all panels) visible in the satellite image.

A few moraine units in the far eastern portion of the mapping area, between Lucia Glacier and Bancas Point, were mapped as undifferentiated (Qbu) because they differ from other moraines in the

mapping area by occurring on relatively steep mountain slopes supporting unique vegetation that precludes the use of forest cover as a determinant of relative moraine age.

Relative ages of mapped moraine deposits and of inferred historic ice extents do not necessarily map to specific glacier advances. The one exception is the boundary of the 1986–87 surge near Malaspina Lake, which is well documented in the satellite record and is described by Muskett et al. (2008). The other moraines and advance margins are significantly older. We provide no new dates, but generally concur with Plafker and Miller (1958) and others, as cited below, in their interpretations of the sources and ages of those features. Briefly, those include:

- The 'older ice extent' in the eastern part of the study area near Point Manby marks the advance of Hubbard Glacier into Yakutat Bay between 970–1290 AD (Barclay et al. 2001). The 'older ice extent' in the western part of the study area near Yana Stream marks the advance of the Yahtse Glacier into Icy Bay between 600–920 AD (Barclay et al. 2006). We note that sequential elevation models, including the 2020 lidar, suggests that there may still be buried Hubbard Glacier ice slowly thawing and subsiding near Point Manby.
- The 'young ice extent' in the eastern part of the study area near Blizhni Point marks the advance of Hubbard Glacier to about Blizhni Point between 1700–1791 AD. The 'young ice extent' in the western part of the study area near Riou Bay marks the advance of the Yahtse Glacier to that area sometime before 1794 AD (Barclay et al. 2006).
- The roughly coast-parallel 'young' ice extent between Point Manby and Sudden Stream marks the maximum advance of Seward Lobe of Sít' Tlein sometime approximately concurrent with the stagnation of the Hubbard and Yahtse Glaciers in the 19th century. One interesting detail revealed in our lidar imagery southwest of Malaspina Lake and west of Forney Stream is the presence of subglacial flutes trending roughly perpendicular to each other (Figure 5). We interpret the S-trending landforms as subglacial bedforms deposited by a Sít' Tlein advance. That advance overrode—but in some cases preserved—WSW-trending landforms that were deposited by the older Hubbard Glacier advance.
- One area where our mapping disagrees with Plafker and Miller's is near Point Riou, where they mapped features west of the Yahtse River outwash as dunes. Instead, we interpret fluted landforms underneath the forest cover as older moraine (Qm2) deposited by an earlier glacier advance of glaciers from Icy Bay and overlain to the northwest by the terminal moraine (Qm1) of a younger Icy Bay advance.
- We see no evidence of, and do not show in our map, deposits associated with a ~60 km^2 lake purportedly mapped by early Russian explorers near the lowermost suture between the Seward and Agassiz Lobes. This feature, as interpreted by Gaglioti et al. (2019), was presumably overridden by a subsequent glacier advance and is now beneath the modern ice, upstream of the present margin.

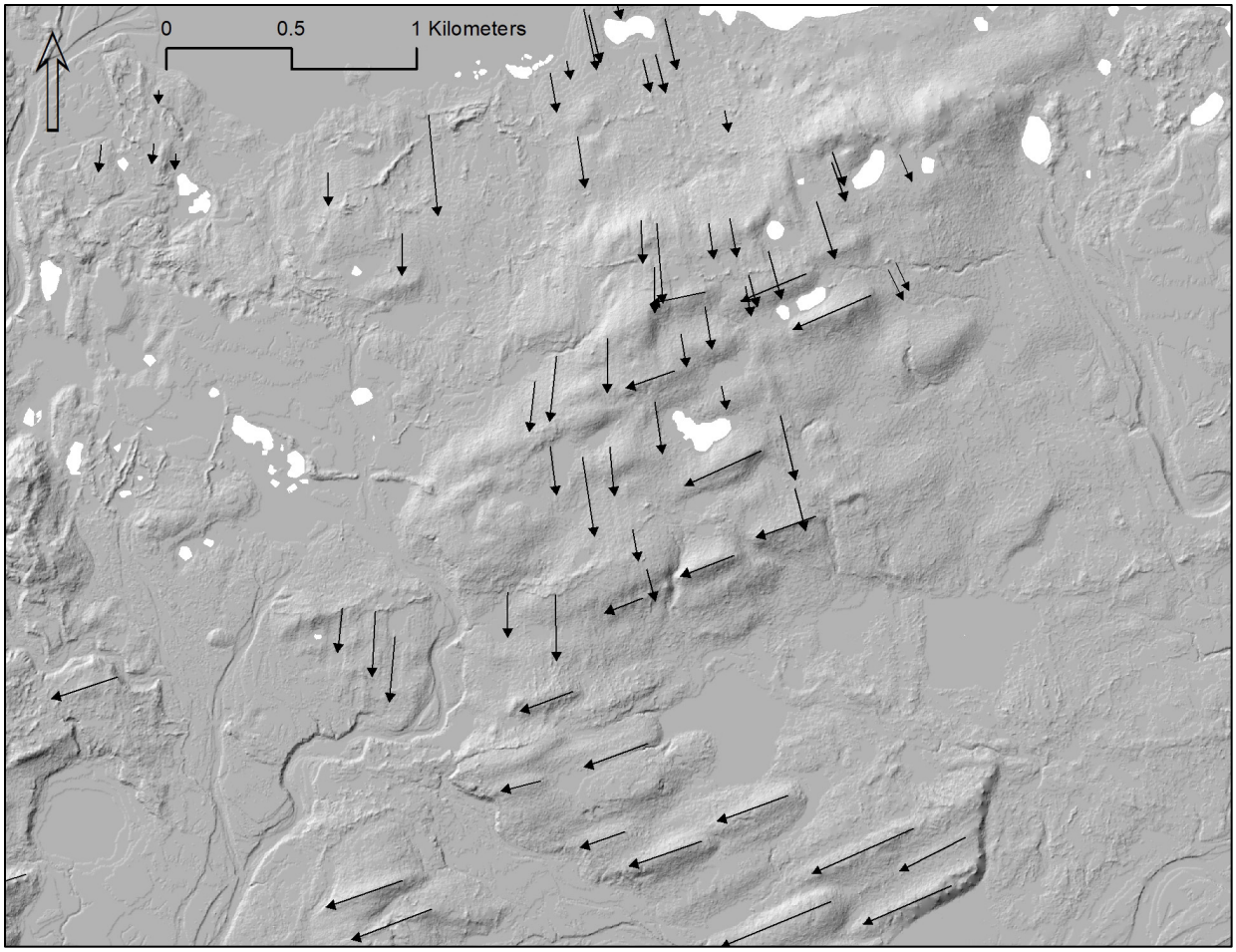

Figure 5. Flowline annotations on a lidar-based bare earth hillshade base map. We interpret the north-south landforms as subglacial landforms indicative of southward flowing Sít' Tlein ice that overrode older east-west landforms indicative of a prior WSW flowing advance of Hubbard Glacier. Area shown is west of Forney Stream and south of Malaspina Lake.

The least abundant types of landforms mapped were the different types of marine beach, bar, and spit deposits. These are all naturally close to the coast and collectively cover less than 2% of the study area. They were generally easy to distinguish from other landforms by their coast-parallel orientations, except in the area east of Point Manby where fluted moraines from the older Hubbard Glacier advance are coincidentally coast-parallel. Where coastal units were large enough to map at 1:24,000 and dominantly terrestrial, we mapped them as younger (Qb2-basically modern coastline features) or older (Qb1) on the basis of vegetation cover, as we did with moraines and outwash deposits. Where they consisted of a closely packed set of upland features alternating with topographically lower areas inundated or at least periodically saturated by a variable mix of seawater and freshwater, we collectively mapped them as packages of Marine Beach, Bar, and Lagoon Deposits, Undifferentiated (Qbu).

Qbu can extend further inland than might be otherwise expected (e.g., >4 km in low relief terrain at Blizhni Point). We interpret these higher features (up to about 16 masl) as raised shorelines

attributable primarily to periodic coseismic uplift of up to 14 m per event (Tarr and Martin 1912, Walton et al. 2022). A minor uplift contribution can also be attributed to isostatic uplift raising the foreland beaches at 20–24 mm/yr (Larsen et al. 2005). Patterns of erosion and deposition, especially near Point Manby, suggest that the highest shorelines are younger than the Hubbard Glacier advance but older, and hence crosscut by, moraines and outwash from the most recent ('young' in our mapping) Sít' Tlein advance.

One area of notable coastal change is in the western portion of the mapping area, where the shape and possibly location of Point Riou Spit and Tsimpshian Point have apparently changed dramatically since 1958. It appears that the entire foreland shoreline has changed since 1958, but magnitudes of absolute change in shoreline *position* are difficult to assess because there are neither reliable benchmarks nor truly stable terrain with which to unequivocally co-register modern and older maps. For this reason, it is beyond the scope of this project to do a quantitative assessment of coastline change along the foreland. At Riou Spit, however, apparent northward migration of the shoreline and a substantial change in the *shape* of the spit (which could only trivially be impacted by georeferencing errors; Figure 6) confirm, at least for this location, substantial shoreline changes. Coastal processes, especially including changes in longshore transport and reduced sediment supply from the abandonment of the Yahtse River outlet to the west, are likely responsible for much of the observed change. Further to the east, a historic photo from the early 1900s (Figure 7) suggest the Sitkagi Bluffs were debris-covered ice directly in contact with tidewater (Tarr and Cornell University Library, 2014). The shoreline position has probably retreated in that area due to subsequent retreat and stabilization of the glacier margin, but because of the georectification challenges described above we do not attempt to further quantify that change.

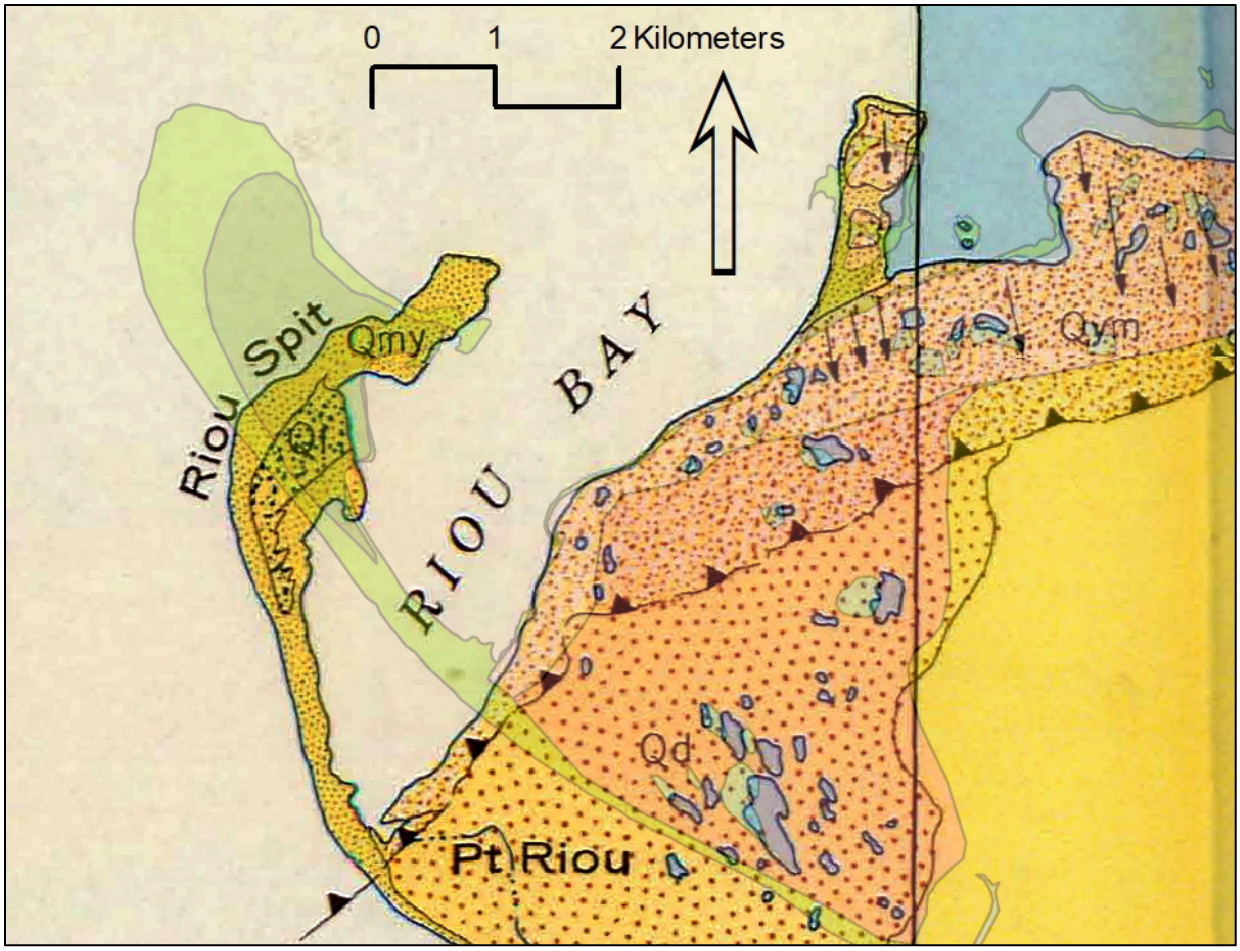

Figure 6. Our map of Riou Spit transparently overlying Plafker and Miller's 1958 map of the same area. The modern spit outline (in green) is substantially north of the 1958 location. Georeferencing errors could be contributing to that offset, but also note the change in shape.

Figure 7. Undated photograph of Sitkagi Bluffs, looking east, taken by Ralph Tarr sometime between 1905 and 1911 (Tarr and Cornell University Library, 2014). Morphology visible in the photos strongly suggests that the bluffs consisted of debris-covered ice at this time.

Proglacial Lake Outlines

The time series of lake outlines derived from Landsat scenes 1972–2020 are shown at varying scales in Figures 8–11. The legends for each map key outline color to the reference year, but we refer the reader to Table 3 as a reminder that not all lakes were actually digitized in a given region for each year. Only lakes within the Central Zone (Figures 9 and 10) are mapped for all years shown in the legend. All four maps are plotted on a hillshade image of the 2012 IFSAR DTM, and the maps are presented in order from east to west, reserving Sitkagi Lagoon for the greatest level of detail.

Over the breadth of the Seward Lobe, the temporal pattern of change in lake-covered area was dominated by the shrinkage and then regrowth of Malaspina Lake in response to the 1986–87 surge of the Seward Lobe terminus into the lake (Figures 8 and 12). Gradual retreat of that surge margin started around 1988 and continued until cumulative lake area returned to the pre-surge value of ~100 km^2 by 2005. The far southeastern corner of Malaspina Lake is an exception to this regrowth of the lake margin after the surge; a supraglacial stream draining the central Marvine Lobe began building a fan delta in that shallow area after the surge, and growth of that delta has been narrowing the primary lake outlet at Sudden Stream since that time. Figure 8 also shows the rapid increase in the number of small proglacial (and supraglacial) lakes west and southwest of Malaspina Lake starting around 2005.

Figure 12 shows that the number of lakes in the overall foreland continued a gradual climb through the entire study interval, mostly unaffected by the 1986–87 surge, starting with only 10 proglacial lakes in 1972 and culminating with 246 lakes in 2020. We acknowledge that the poor quality and resolution of early Landsat imagery likely caused an undercount of the very smallest early lakes and thus biased the early lake count towards lower totals relative to the modern era, but argue later in this report that the strong trend of growth in lake numbers over time is real. Increasingly large numbers of new lakes appeared in the western portion of Seward Lobe around Fountain Stream (Figure 11) and, as already mentioned, in the area west of Malaspina Lake (Figure 8).

Lake area and number change in the Central Zone (only) is shown in Figure 13. We digitized lake boundaries at higher temporal resolution in the Central Zone primarily because Sitkagi Lagoon is immediately adjacent to the coastal beach and appears to be receiving at least occasional saltwater from the adjacent ocean during high tides (Thompson et al. 2021). This situation introduces the potential for enhanced retreat rates because of tidewater glacier dynamics and heightens both the importance of Sitkagi Lagoon's geometric configuration and the pattern of past and potential future connection to other water bodies like Backdoor Lake. Patterns of lake change in the Central Zone generally mimic those seen elsewhere, but without the significant impact of the 1986–87 surge, which minimally impacted this area. Lake numbers increased from 2 to a maximum of 30, and lake area doubled from about 3 to more than 6 km^2 (Figure 13).

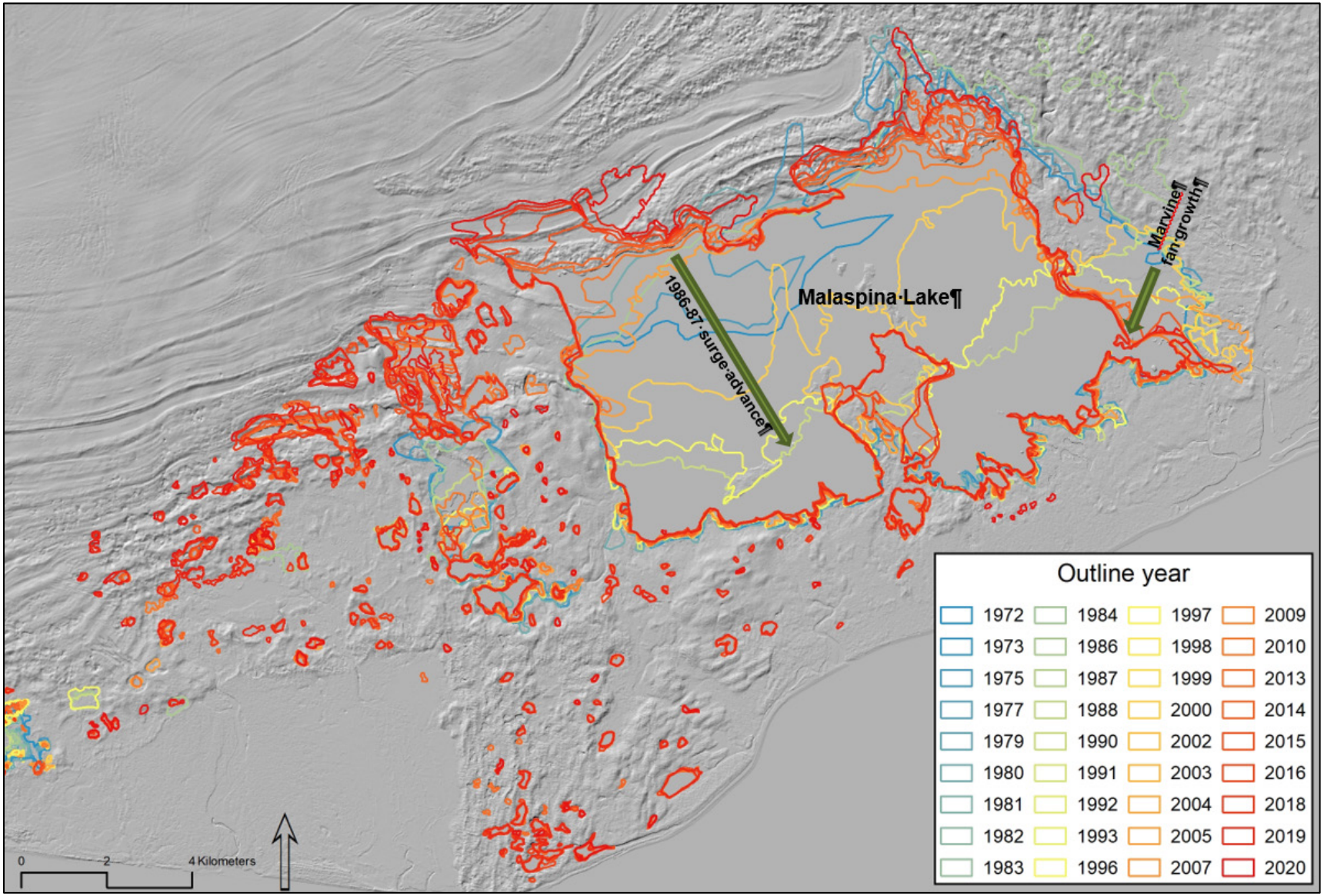

Figure 8. Lake outlines from eastern Seward Lobe and Malaspina Lake 1972–2020. Note scale varies among these maps.

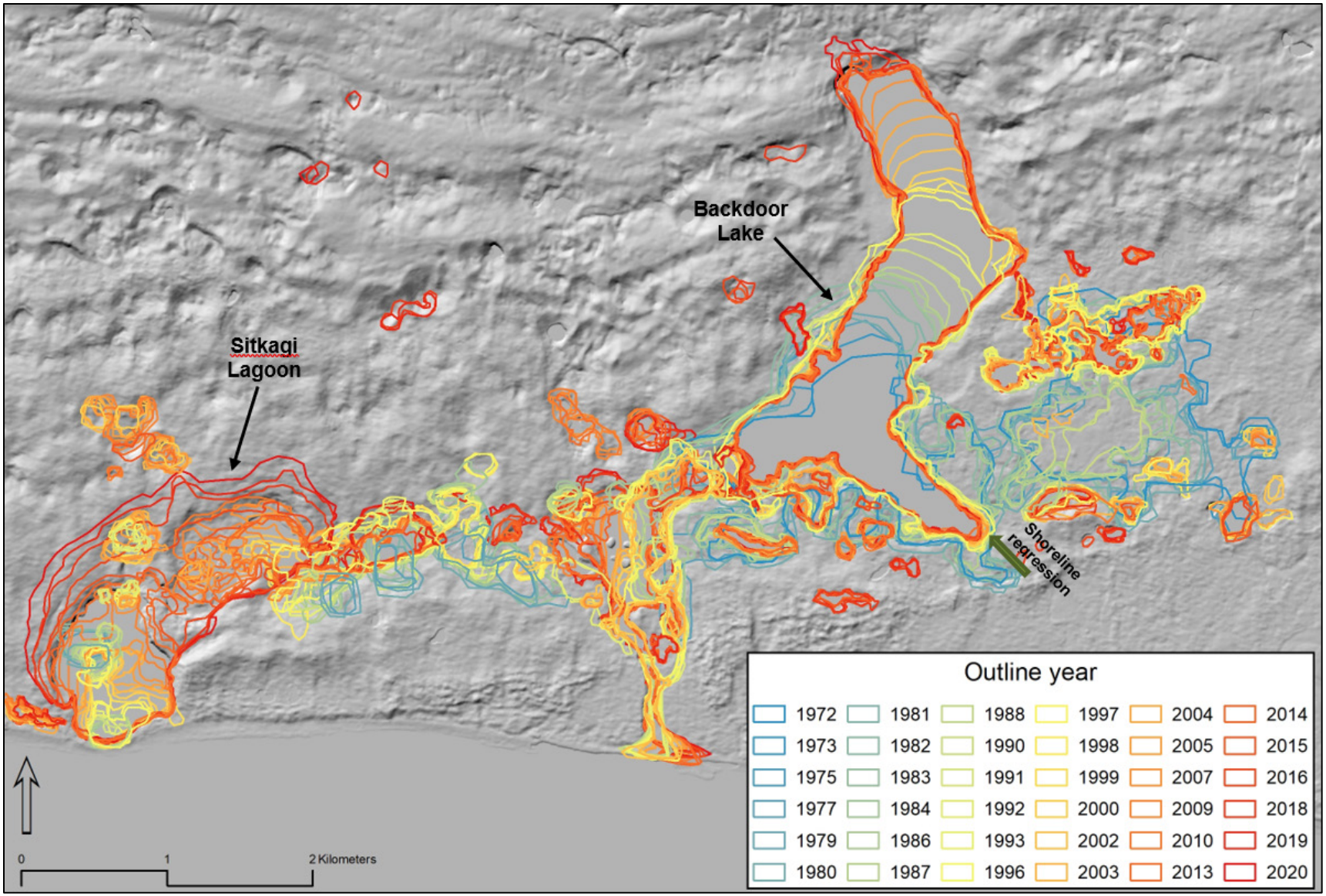

Figure 9. Lake outlines from Central Zone (Sitkagi Lagoon and Backdoor Lake) 1972–2020. Note scale varies among these maps.

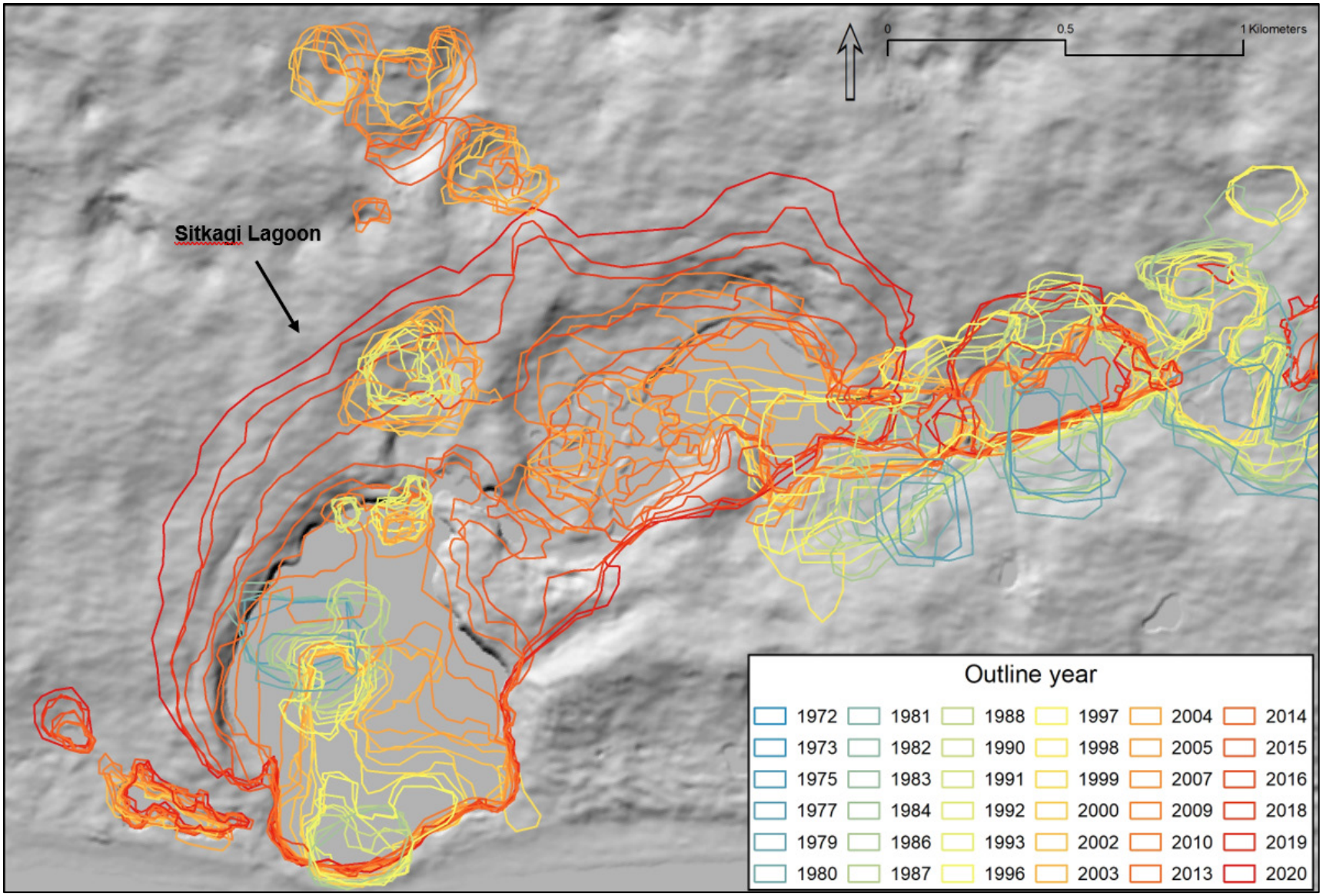

Figure 10. Lake outlines from the Sitkagi Lagoon area 1972–2020. Note scale varies among these maps.

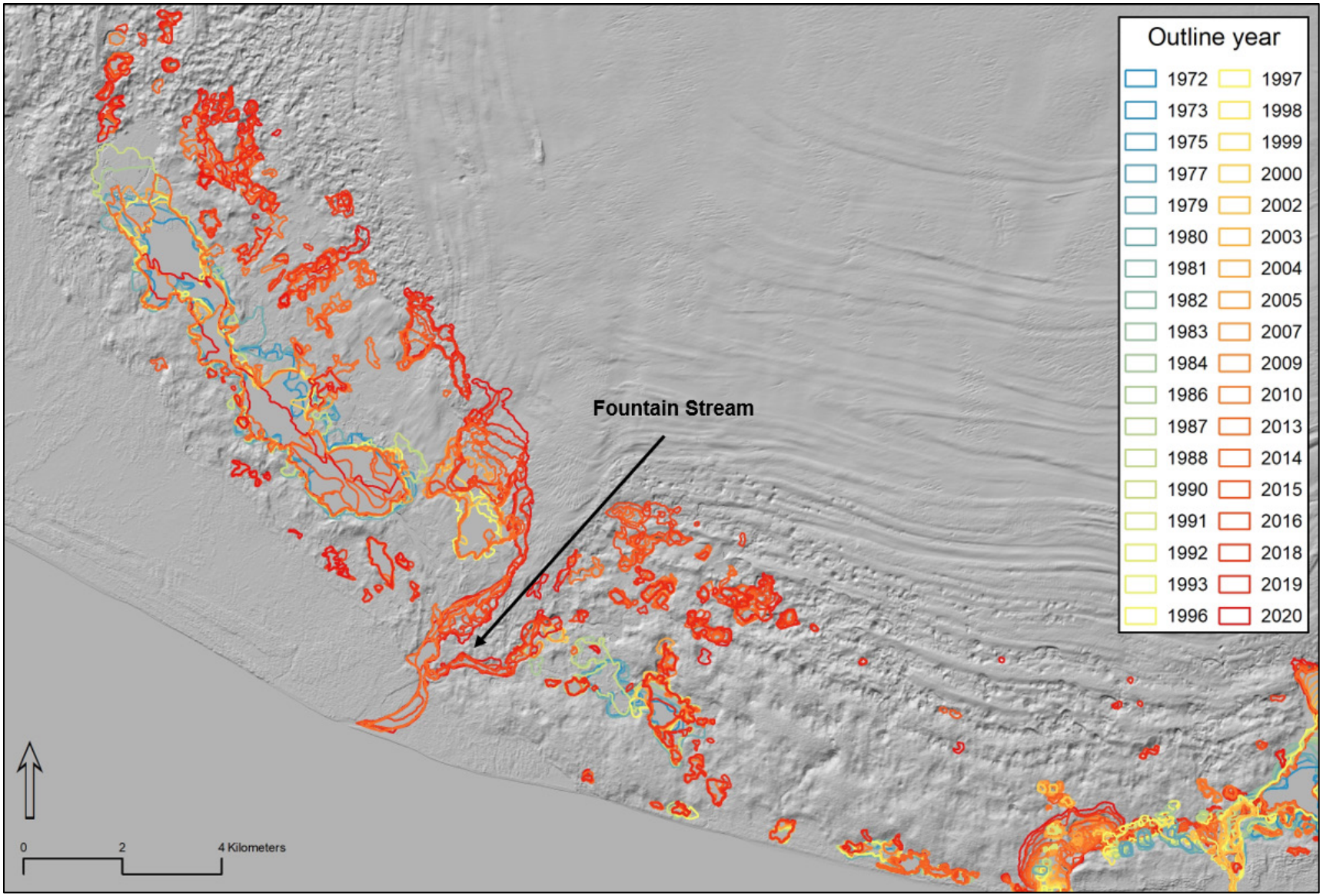

Figure 11. Lake outlines from the western portion of the Seward Lobe 1972–2020. Note scale varies among these maps.

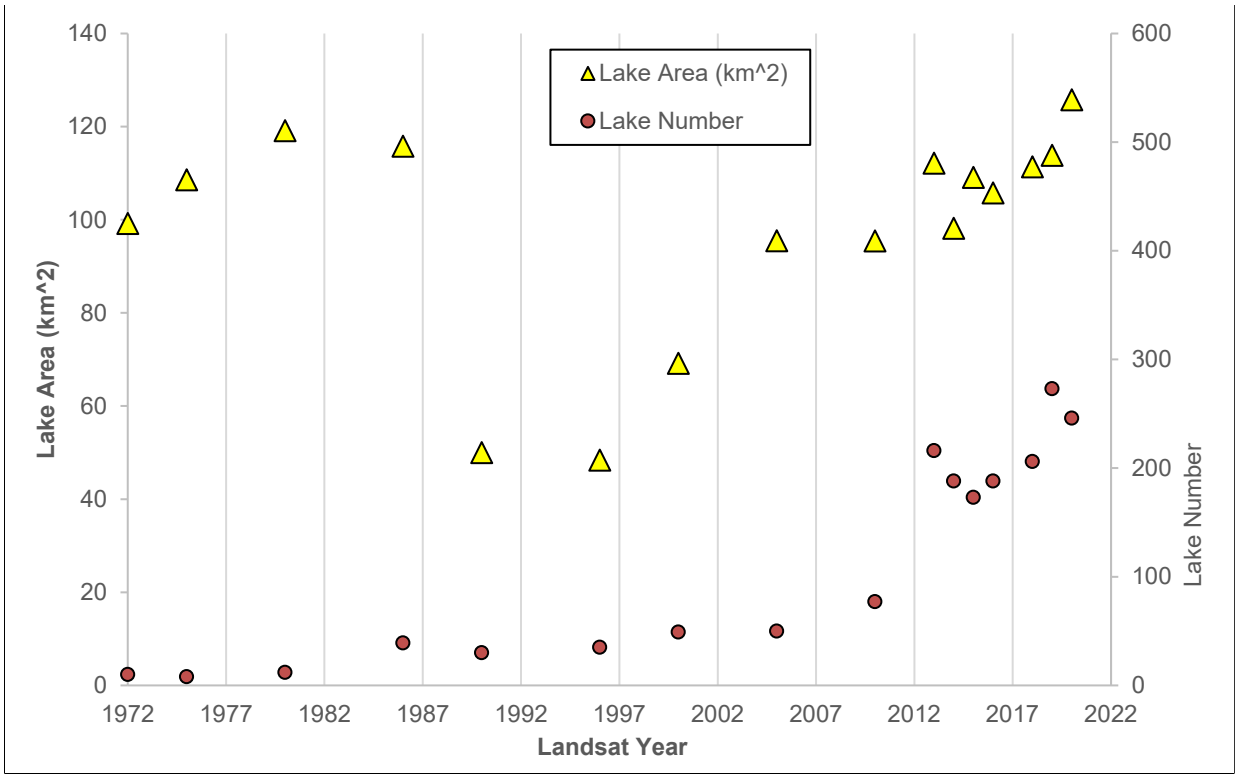

Figure 12. Evolution of lake number and area over the entire Seward Lobe for selected years, 1972–2020.

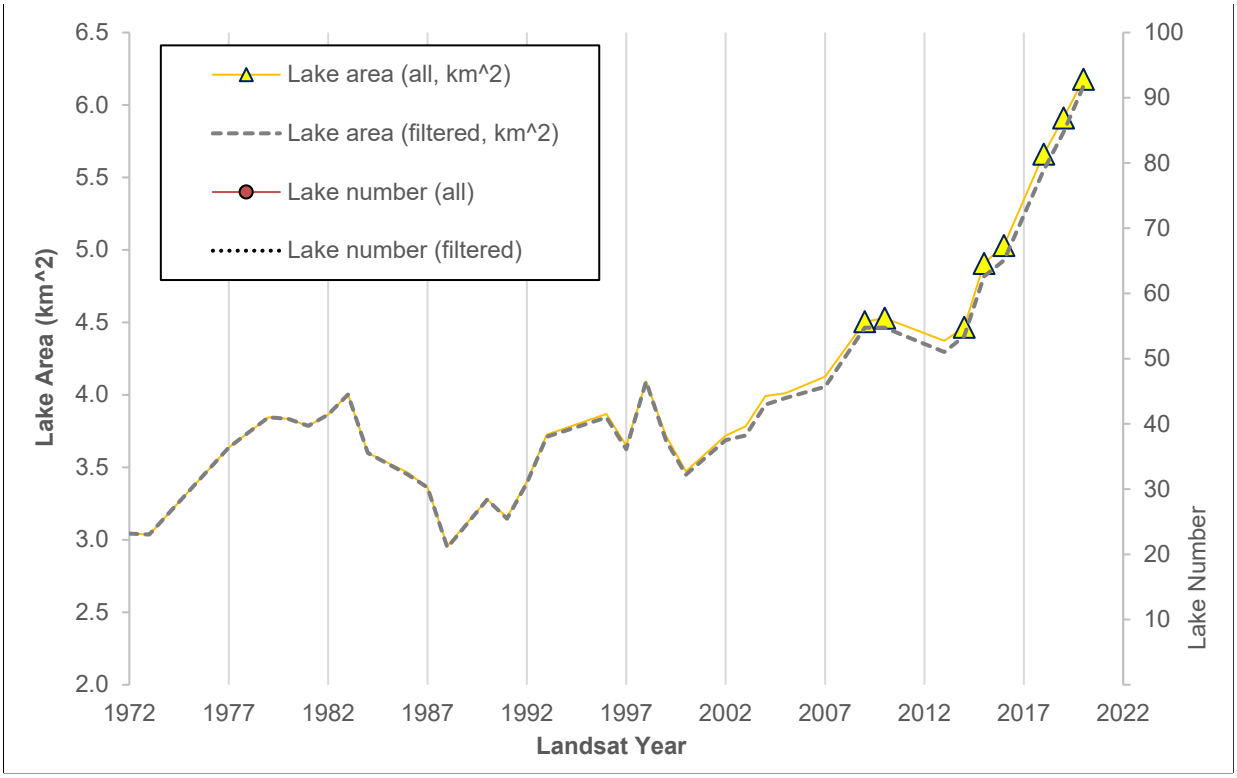

Figure 13. Evolution of lake number and area within the Central Zone only, 1972–2020. Dashed lines show results for the same area when filtered to include only lakes larger than 0.014 km^2, equivalent to four 60 m pixels in earliest Landsat imagery. Note that y axes differ from Figure 12 for this smaller sample area.

As in the broader study area, increase in the number of lakes in the Central Zone is not monotonic, and lake numbers dropped slightly in some years. Some of these small drops might be due to the imagery-related biases and errors already mentioned, and to examine that possibility we filtered the dataset to exclude small lakes under 0.014 km^2 in area, the equivalent of four 60 m pixels in the earliest Landsat imagery (Figure 13). Total lake area is barely affected by this filter, but lake numbers rise more gradually and actually decline somewhat after 2007. Still, even with the filtering the lake numbers in the central area rise from two to 15 over the sampling interval, indicating that the trend of lake growth is likely real, despite the image resolution bias. Occasional reductions in lake number (whether in the full dataset or the filtered one) probably sometimes also reflect the fact that some of the larger lakes in the study area have grown through the coalescence of multiple smaller lakes. Sitkagi Lagoon, shown in Figure 8 and Figure 9, provides a good example. Numerous small thermokarst lakes formed independently in that area between 1972 and about 2013; around 2013, many of these smaller lakes began to coalesce. Analogous joining events contributed at various times and places towards minor reductions in lake numbers.

Coalescence of independent thermokarst lakes also explains the pattern, in some areas, of progressive lake margin retreat—a process that seems at first to contradict the broader pattern of lake growth and development. One example is shown in Figure 8 at the end of the NW/SE trending arm at the SE end

of Backdoor Lake. Despite overall growth of the lake, the shoreline of that particular arm clearly retreats into deeper water between the 1970s/80s and the present. We explain this and similar observations elsewhere as a consequence of dropping base levels. As isolated thermokarst lakes gradually connect to other lakes, providing them with new outlets that drain ultimately towards the ocean, lake levels will sometimes drop. Unless subsurface thaw and continued thermokarst development compensates for that lake level drop, the consequence is shoreline regression. The same process probably explains the occasional disappearance of thermokarst lakes through complete drainage by new outlets. This evidence for sporadically dropping lake levels supports our inference that the overall trend of growth in size of bigger lakes like Sitkagi, Backdoor, and Malaspina is mainly due to thaw-induced shoreline degradation and is not a consequence of regionally rising water levels.

Conclusions

We have produced a new surficial geologic map of the Sít' Tlein foreland and supplemented that map with a time-series of Landsat-based proglacial lake outlines from 1972–2020. Despite evidence for significant downwasting of the glacier surface in recent decades (Loso et al. 2014, Larsen et al. 2015), and also for a significant surge event in 1986–87 (Muskett et al. 2008, Devaux-Chupin et al. 2021), the glacier boundary and foreland surficial geology has overall evolved very little since an earlier geologic map was completed in 1958 (Plafker and Miller).

Our mapping units and source imagery differ from those of Plafker and Miller (1958), but taking those differences into account, the foreland (on and downstream of the glacier terminus) has remained surprisingly stable. Surficial deposits continue to be dominated by outwash of present and former glacial streams, by end moraines and subglacially streamlined till, and by coastal beaches and spits. Vegetation cover on many of those landforms, including debris-covered ice upstream of the glacier terminus, thickened and spread in many cases.

Evidence from our mapping and from that of past investigators (e.g., Plafker and Miller 1958, Barclay et al. 2001, Barclay et al. 2006) confirms that the past ~century of relative stability for the glacier and for the thin shield of proglacial landforms that protect it from tidal influence of the adjacent Pacific Ocean is relatively anomalous from the perspective of late Holocene glacial history. Several cycles of advance and retreat by neighboring glaciers to the west (Yahtse Glacier) and east (Hubbard Glacier) have repeatedly connected those glacier termini with that of Sít' Tlein. We know this not only from the work of western scientists but also from the oral history of Tlingit neighbors who use the same name, Sít' Tlein, for both Hubbard and Malaspina Glaciers. Though that shared name may have other origins, we interpret it as consistent with the argument that those two glaciers, though today separated by over 30 km, were once united by a single ice front.

Our maps reveal one significant progressive change in the Sít' Tlein foreland: the growth of proglacial and minor supraglacial lakes. The largest lake in the foreland, Malaspina Lake, has been very long-lived and persistent even through a substantial disruption by the 1986–87 surge. However, early 1970s Landsat imagery confirms that there were very few other lakes in the foreland. The emergence, growth, and interconnection of thermokarst lakes since that time has resulted in the creation of well over 200 new lakes. Most are small relative to Malaspina Lake, but they are with few exceptions ice-walled and hence capable of accelerating degradation of the glacier terminus by subaqueous melt and calving. One of them, Sitkagi Lagoon, is immediately adjacent to, and receiving sporadic saltwater inputs from, the Pacific Ocean (Thompson et al. 2021), potentially enhancing opportunities for melt, calving, and initiation of catastrophic tidewater glacier retreat (Post et al. 2011). Our mapping, in other words, documents a recent period of relative stability but depicts trends in lake development that might portend a more dynamic future.

Literature Cited

Barclay, D. J., Barclay, J. L., Calkin, P. E., Wiles, G. C. 2006. A revised and extended Holocene glacial history of Icy Bay, southern Alaska, USA. Arctic, Antarctic, and Alpine Research 38:153–162.

Barclay, D. J., Calkin, P. E., Wiles, G. C. 2001. Holocene history of Hubbard Glacier in Yakutat Bay and Russell Fiord, southern Alaska. Geological Society of America Bulletin 113:388–402.

Conway, H., Smith, B., Vaswani, P., Matsuoka, K., Rignot, E., Claus, P. 2009. A low-frequency ice-penetrating radar system adapted for use from an airplane: test results from Bering and Malaspina Glaciers, Alaska, USA. Annals of Glaciology 50:93–97.

Cotton, M. M., Bruhn, R. L., Sauber, J., Burgess, E., Forster, R. R. 2014. Ice surface morphology and flow on Malaspina Glacier, Alaska: Implications for regional tectonics in the Saint Elias orogen: Malaspina Glacier, Alaska. Tectonics 33:581–595.

Cruikshank, J. 2001. Glaciers and climate change: perspectives from oral tradition. Arctic 54:377–393.

Devaux-Chupin, V., Fahnestock, M., Truffer, M., Holt, J., Loso, M., Jones, T., Christoffersen, M., Kuehn, T., Thompson, A., Tober, B., and Wagner, N. 2021. Ice-flow and surge history of the Malaspina Glacier, Alaska, from Landsat and Sentinel data, and autonomous repeat image feature tracking (autoRIFT). AGU Fall Meeting Abstracts 2021:C13B-03.

Elmore, C. R., Gulick, S. P. S., Willems, B., Powell, R. 2013. Seismic stratigraphic evidence for glacial expanse during glacial maxima in the Yakutat Bay Region, Gulf of Alaska. Geochemistry, Geophysics, Geosystems 14:1294–1311.

Fickert, T., Friend, D., Grüninger, F., Molnia, B., Richter, M. 2007. Did Debris-Covered Glaciers Serve as Pleistocene Refugia for Plants? A New Hypothesis Derived from Observations of Recent Plant Growth on Glacier Surfaces. Arctic, Antarctic, and Alpine Research 39:245–257.

Fickert, T., Friend, D., Molnia, B., Grüninger, F., Richter, M. 2022. Vegetation Ecology of Debris-Covered Glaciers (DCGs)—Site Conditions, Vegetation Patterns and Implications for DCGs Serving as Quaternary Cold- and Warm-Stage Plant Refugia. Diversity 14:114.

Ford, A. L., Forster, R. R., Bruhn, R. L. 2003. Ice surface velocity patterns on Seward Glacier, Alaska/Yukon, and their implications for regional tectonics in the Saint Elias Mountains. Annals of Glaciology 36:21–28.

Fugro Earthdata. 2016. ORI_N5945W14030, 1st Edition. Available at: https://earthexplorer.usgs.gov (accessed 15 January 2019). DOI:10.5066/F7CJ8CSF.

Gaglioti, B. V., Mann, D. H., Wiles, G. C., Jones, B. M., Charlton, J., Wiesenberg, N., Andreu-Hayles, L. 2019. Timing and potential causes of 19th-century Glacier Advances in Coastal Alaska Based on Tree-Ring Dating and Historical Accounts. Frontiers in Earth Science 7(82):1–15.

Gustavson, T. C., 1974. Sedimentation on Gravel Outwash Fans, Malaspina Glacier Foreland, Alaska. Journal of Sedimentary Petrology 44(2):374–389.

Gustavson, T. C. 1975a. Bathymetry and Sediment Distribution in Proglacial Malaspina Lake, Alaska. Journal of Sedimentary Petrology 45(2):450–461.

Gustavson, T.C., 1975b. Sedimentation and physical limnology in proglacial Malaspina Lake, southeastern Alaska. Pages 249–362 *in* Jopling, A.V., McDonald, B.C., editors, Glaciofluvial and Glaciolacustrine Sedimentation, Special Publication. Society of Economic Paleontologists and Mineralogists, Tulsa, Oklahoma.

Larsen, C. F., Motyka, R. J., Freymueller, J. T., Echelmeyer, K. A., Ivins, E. R. 2005. Rapid viscoelastic uplift in southeast Alaska caused by post-Little Ice Age glacial retreat. Earth and Planetary Science Letters 237:548–560.

Larsen, C. F., Burgess, E., Arendt, A. A., O'Neel, S., Johnson, A. J., Kienholz, C. 2015. Surface melt dominates Alaska glacier mass balance. Geophysical Research Letters 42:5902–5908.

Loso, M. G., Arendt, A. A., Larsen, C. F., Rich, J. L., Murphy, N. 2014. Alaskan National Park Glaciers-status and trends: Final report. Natural Resource Technical Report No. NPS/AKR/NRTR-2014/922. National Park Service, Fort Collins, Colorado.

Luthcke, S. B., Arendt, A. A., Rowlands, D. D., McCarthy, J. J., Larsen, C. F. 2008. Recent glacier mass changes in the Gulf of Alaska region from GRACE mascon solutions. Journal of Glaciology 54:767–777.

Miller, D. J. 1961. Geology of the Malaspina District, Gulf of Alaska Tertiary Province, Alaska. U.S. Geological Survey Preliminary Map.

Muskett, R. R., Lingle, C. S., Sauber, J. M., Post, A. S., Tangborn, W. V., Rabus, B. T. 2008. Surging, accelerating surface lowering and volume reduction of the Malaspina Glacier system, Alaska, USA, and Yukon, Canada, from 1972 to 2006. Journal of Glaciology 54:788–800.

Muskett, R. R., Lingle, C. S., Tangborn, W. V., Rabus, B. T. 2003. Multi-decadal elevation changes on Bagley ice valley and Malaspina Glacier, south-central Alaska. Tohoku Geophysical Journal 36:422–424.

Plafker, G., Miller, D. J. 1958. Glacial features and surficial deposits of the Malaspina District, Alaska. U.S. Geological Survey Miscellaneous Geologic Investigations Map I-271.

Post, A., O'Neel, S., Motyka, R. J., and Streveler, G. 2011. A complex relationship between calving glaciers and climate. Eos, Transactions, American Geophysical Union 92:305–306.

Pfeffer, W. T. and others. 2014. The Randolph Glacier Inventory: a globally complete inventory of glaciers. Journal of Glaciology 60:537–552.

Richter, D. R., Preller, C. C., Labay, K. A., Shrew, N. B. 2006. Geologic Map of the Wrangell-Saint Elias National Park and Reserve, Alaska. U.S. Geological Survey Scientific Investigations Map 2877.

Rignot, E., Mouginot, J., Larsen, C. F., Gim, Y., Kirchner, D. 2013. Low-frequency radar sounding of temperate ice masses in Southern Alaska. Geophysical Research Letters 40:5399–5405.

Russell, I. C. 1891. An expedition to Mount St. Elias, Alaska. National Geographic Magazine 3:53–204.

Sauber, J. 2005. Ice elevations and surface change on the Malaspina Glacier, Alaska. Geophysical Research Letters 32:1–4.

Sharp, R. P. 1951. Accumulation and ablation on the Seward-Malaspina Glacier system, Canada-Alaska 62:725–744.

Sharp, R. P. 1958a. The latest major advance of Malaspina Glacier, Alaska. Geographical Review 48:16–26.

Sharp, R. P. 1958b. Malaspina Glacier, Alaska. Geol Soc America Bull 69:617–646.

Tarr, R. S., Martin, L. 1912. The earthquakes at Yakutat Bay, Alaska, in September, 1899. U.S. Geological Survey Professional Paper 69.

Tarr and Cornell University Library. 2014. Historic Glacial Images of Alaska and Greenland. Available at: http://digital.library.cornell.edu/collections/tarr (accessed 30 March 2023). https://doi.org/10.7298/X4M61H5R

Tebenkov, M. D. 1852. Atlas of the northwest coast of America from the Bering Strait to Corroentes and the Aleutian Island. Chart VII. Available at: geoportal.rgo.ru/record/6874 (accessed 15 March 2023).

Thompson, A., Loso, M., Jones, T., Truffer, M., Holt, J., Devaux-Chupin, V., Tober, B., Christoffersen, M., Kuehn, T., Wagner, N. and Fahnestock, M. 2021. Saltwater Intrusion in Proglacial Lakes at Malaspina Glacier, Southeast Alaska: Introducing the World's Newest Tidewater Glacier. AGU Fall Meeting Abstracts 2021:C13B-07.

Thornton, T. F. 2012. Haa Leelk'w Has Aani Saaxu / Our Grandparents Names on the Land. University of Washington Press, Seattle, Washington.

Tober, B. S., Holt, J. W., Christoffersen, M. S., Truffer, M., Larsen, C. F., Brinkerhoff, D. J., and Mooneyham, S. A. 2023. Comprehensive Radar Mapping of Malaspina Glacier (Sít' Tlein), Alaska—The World's Largest Piedmont Glacier—Reveals Potential for Instability. Journal of Geophysical Research: Earth Surface 128(3). https://doi:10.1029/2022JF006898

Walton, M. A. L., Gulick, S. P. S., Haeussler, P. J. 2022. Revisiting the 1899 earthquake series using integrative geophysical analysis in Yakutat Bay, Alaska, USA. Geosphere 18:1453–1473.

Windnagel, A., Hock, R., Maussion, F., Paul, F., Rastner, P., Raup, B., Zemp, M. 2022. Which glaciers are the largest in the world? Journal of Glaciology 1–10. https://doi.org/10.1017/jog.2022.61

Zurbuchen, J. M., Gulick, S. P. S., Walton, M. A. L., Goff, J. A. 2015. Imaging evidence for Hubbard Glacier advances and retreats since the last glacial maximum in Yakutat and Disenchantment Bays, Alaska. Geochemistry, Geophysics, Geosystems 16:1962–1974.

The Department of the Interior protects and manages the nation's natural resources and cultural heritage; provides scientific and other information about those resources; and honors its special responsibilities to American Indians, Alaska Natives, and affiliated Island Communities.

NPS 190/192381, January 2023

Natural Resource Stewardship and Science
1201 Oakridge Drive, Suite 150
Fort Collins, CO 80525